Available online at www.sciencedirect.com
ScienceDirect
Journal of Sound and Vibration 322 (2009) 314–335
JOURNAL OF SOUND AND VIBRATION
www.elsevier.com/locate/jsvi

On nonlinear vibrations of a rotating beam

Özgür Turhan*, Gökhan Bulut

Faculty of Mechanical Engineering, Istanbul Technical University, Gümüşsuyu 34437, Istanbul, Turkey

Received 25 January 2008; received in revised form 4 November 2008; accepted 4 November 2008
Handling Editor: M.P. Cartmell
Available online 1 January 2009

Abstract

In plane nonlinear bending vibrations of a rotating beam is studied. The equation of motion is obtained in the form of an integro-partial differential equation and then discretized by means of Galerkin's method. Perturbation analyses are performed on single- and two-degree-of-freedom models to obtain amplitude dependent natural frequencies and frequency responses. Results are presented for the first two modes.

1. Introduction

Vibrations of rotating blades or beams have been a subject of constant research interest since about a century [1]. Along with many studies treating the problem through linear models (see Refs. [2–6] for example), there are a number of studies treating the effect of nonlinearities. Rao and Carnegie [7,8] studied the in plane free and forced vibrations of a rotating beam under the nonlinear effect of Coriolis forces by using the Ritz method. Ansari [9,10] treated the same problem by means of a discrete model. Gross et al. [11] and Brons and Kliem [12] studied the buckling problem of inward-oriented rotating nonlinear beams. Peshek et al. [13] applied the nonlinear modal reduction concept to the study of coupled extensional-transversal vibrations of a rotating beam with nonlinear axial strain. Abolghasemi and Jalali [14] considered a similar coupled problem for a beam with periodically varying pitch angle and have shown by means of Poincaré maps that the system may exhibit chaotic behaviour. Hamdan and Al-Bedoor [15] studied the free vibrations of a rotating beam with nonlinear curvature via a single-degree-of-freedom (dof) model by using a time transformation method. Finally, Larsen and Nielsen developed a nonlinear model for the coupled in and out of plane bending vibrations of pre-twisted wind turbine blades with periodically moving support [16], and used a two-dof reduced form of that model to construct stability/chaos charts of the system via Lyapunov exponent calculations [17]. A similar problem was also addressed by Bulut and Turhan [18] who have worked out chaos charts for the in plane vibrations of a rotating beam with periodically varying speed, through a single-dof model.

The present study treats the in plane vibrations of a rotating Euler–Bernouilli beam with nonlinear curvature. Other nonlinearities of geometric and dynamic origin are also considered up to cubic terms. The

*Corresponding author.
E-mail address: ozgur.turhan@itu.edu.tr (Ö. Turhan).

0022-460X/$ - see front matter © 2008 Elsevier Ltd. All rights reserved.
doi:10.1016/j.jsv.2008.11.012

paper is organized as follows: in Section 2, the nonlinear equation of motion is first obtained in the form of an integro-partial differential equation, and then discretized via Galerkin's method to yield a system of coupled nonlinear ordinary differential equations. Section 3 presents some results obtained through a single-dof model extracted from the general formulation. A qualitative analysis of the singular (equilibrium) points is presented in Section 3.1 and free and forced vibrations are analysed via Lindstedt–Poincaré (LP) method in Sections 3.2 and 3.3, respectively. A two-dof model is then considered in Section 4 where a natural frequency analysis is performed via multiple scales method.

The analyses reveal that a speed change may have some unusual effects on the dynamics of a rotating beam, such as giving rise to a qualitative change from hardening to softening behaviour, and causing harmonic or super-harmonic jump phenomena to occur when the beam is under a periodic excitation of external origin.

2. Equation of motion

Consider a uniform Euler–Bernouilli beam with mass density ρ, cross sectional area A, length ℓ and flexural rigidity EI clamped onto the out or inside of a rigid ring of radius R rotating at constant rate Ω (Figs. 1a and b). To derive the equation of motion governing the in plane transversal vibrations of this system note that a nonlinear integro-partial differential equation for moderately high amplitude transverse vibrations of a stationary Euler–Bernouilli beam with nonlinear curvature, acted upon by a distributed force with components $\bar{f}_x(s,t)$ and $\bar{f}_y(s,t)$ can be written

$$\rho A\left\{\left[1-\frac{1}{2}\left(\frac{\partial y}{\partial s}\right)^2\right]\frac{\partial^2 y}{\partial t^2}+\frac{\partial y}{\partial s}\frac{\partial^2 y}{\partial s^2}\int_s^\ell\frac{\partial^2 y}{\partial t^2}\,d\sigma+\frac{\partial y}{\partial s}\int_0^s\left[\left(\frac{\partial^2 y}{\partial\sigma\,\partial t}\right)^2+\frac{\partial y}{\partial\sigma}\frac{\partial^3 y}{\partial\sigma\,\partial t^2}\right]d\sigma\right.$$
$$\left.-\frac{\partial^2 y}{\partial s^2}\int_s^\ell\int_0^\sigma\left[\left(\frac{\partial^2 y}{\partial\eta\,\partial t}\right)^2+\frac{\partial y}{\partial\eta}\frac{\partial^3 y}{\partial\eta\,\partial t^2}\right]d\eta\,d\sigma\right\}+EI\left[\left[1+\frac{1}{2}\left(\frac{\partial y}{\partial s}\right)^2\right]\frac{\partial^4 y}{\partial s^4}+3\frac{\partial y}{\partial s}\frac{\partial^2 y}{\partial s^2}\frac{\partial^3 y}{s^3}+\left(\frac{\partial^2 y}{\partial s^2}\right)^3\right]$$
$$-\frac{\partial^2 y}{\partial s^2}\int_s^\ell\bar{f}_x(\sigma,t)\,d\sigma-\frac{\partial y}{\partial s}\frac{\partial^2 y}{\partial s^2}\int_s^\ell\bar{f}_y(\sigma,t)\,d\sigma+\bar{f}_x(s,t)\frac{\partial y}{\partial s}-\bar{f}_y(s,t)\left[1-\frac{1}{2}\left(\frac{\partial y}{\partial s}\right)^2\right]=0, \tag{1}$$

where up to cubic nonlinearities are considered. (See Appendix A for the derivation of this equation.) Eq. (1) can be used to obtain the equation of motion of the beams of Fig. 1a and b by defining $\bar{f}_x(s,t)$ and $\bar{f}_y(s,t)$ as the corresponding inertia forces due to the rotation of the frame. Considering the outward-oriented beam of Fig. 1a, we set

$$\bar{f}_x(s,t)=\rho A\left\{\Omega^2\left[R+\int_0^s\left(1-\frac{1}{2}\left(\frac{\partial y}{\partial\sigma}\right)^2\right)d\sigma\right]+2\Omega\frac{\partial y}{\partial t}\right\},$$
$$\bar{f}_y(s,t)=\rho A\left\{\Omega^2 y+2\Omega\int_0^s\frac{\partial y}{\partial\sigma}\frac{\partial^2 y}{\partial\sigma\,\partial t}d\sigma\right\}, \tag{2}$$

where recourse has been made to the position and relative velocity vectors given in Eqs. (A.4) and (A.5) of Appendix A. Note that, would the inward-oriented beam of Fig. 1b be considered, $-R$ should replace R in

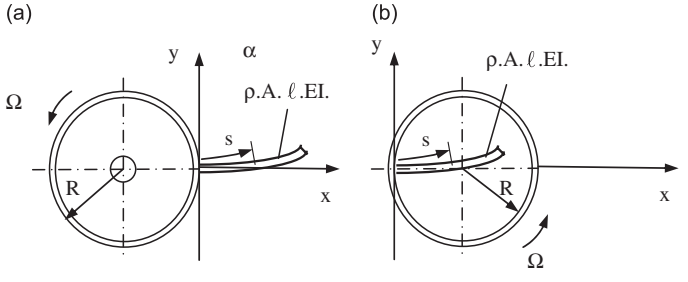

Fig. 1. Rotating beam: (a) oriented outward ($\alpha = R/\ell$); (b) oriented inward ($\alpha = -R/\ell$).

Eq. (2). Substituting Eqs. (2) into Eq. (1), adding linear Kelvin–Voigt material damping with coefficient γ, discarding higher than cubic order terms in consistency with previous omissions, and putting in non-dimensional form, one obtains

$$\ddot{v}+v^{iv}+\zeta\dot{v}^{iv}-\beta^2\left\{\left[\alpha(1-u)+\frac{1}{2}(1-u^2)\right]v''-(\alpha+u)v'+v\right\}+2\beta\cdot\left(\dot{v}v'-v''\int_u^1\dot{v}\,\mathrm{d}\sigma-\int_0^u v'\dot{v}'\right)$$
$$+v'\cdot\left[\int_0^u(v'\ddot{v}'+\dot{v}'^2)\,\mathrm{d}\sigma+v''\int_u^1\ddot{v}\,\mathrm{d}\sigma\right]-v''\cdot\int_u^1\int_0^\sigma(v'\ddot{v}'+\dot{v}'^2)\,\mathrm{d}\eta\,\mathrm{d}\sigma-\frac{1}{2}v'^2\ddot{v}+\frac{1}{2}v^{iv}v'^2+3v'v''v'''+v''^3$$
$$-\beta^2\left(\frac{1}{2}v'\int_0^u v'^2\,\mathrm{d}\sigma+v'v''\int_u^1 v\,\mathrm{d}\sigma-\frac{1}{2}v''\int_u^1\int_0^\sigma v'^2\,\mathrm{d}\eta\,\mathrm{d}\sigma-\frac{1}{2}vv'^2\right)=0, \tag{3}$$

where

$$u=\frac{s}{\ell},\quad v=\frac{y}{\ell},\quad \alpha=\frac{R}{\ell},\quad \tau=\omega^* t,\quad \beta=\frac{\Omega}{\omega^*},\quad \zeta=\gamma\omega^*;\ \ \omega^*=\sqrt{\frac{EI}{\rho A\ell^4}}, \tag{4}$$

and primes denote differentiation with respect to u while overdots denoting differentiation with respect to τ. The boundary conditions are

$$v(0,\tau)=v'(0,\tau)=v''(1,\tau)=v'''(1,\tau)=0. \tag{5}$$

Eqs. (3) and (5) constitute a nonlinear boundary value problem for the in plane transverse vibrations of the rotating outward-oriented beam of Fig. 1a. The formulation can as well be used for the inward-oriented beam of Fig. 1b by setting $\alpha=-R/\ell$. Thus, $\alpha\geqslant 0$ will refer to an outward-oriented beam and $\alpha<0$ to an inward-oriented one in the rest of this study. Note that all the nonlinear terms in Eq. (3) are of geometric origin, except the first two Coriolis terms (terms with a factor 2β) that would be present even if geometric nonlinearities were neglected. Note also that Eq. (3) depends only on the two parameters α and β (damping put aside) so that the dynamic character of the system can conveniently be portrayed on a $\alpha-\beta$ plane, as will be done in this study.

The boundary value problem in question can be approximated by a finite set of ordinary differential equations by means of Galerkin's method. To do that, introduce the Galerkin expansion

$$v(u,\tau)=\sum_{i=1}^{n}g_i(\tau)\varphi_i(u) \tag{6}$$

with the eigenfunctions of a linear stationary cantilever as comparison functions

$$\varphi_i(u)=\cosh\,\lambda_i u-\cos\,\lambda_i u-\kappa_i(\sinh\,\lambda_i u-\sin\,\lambda_i u),\quad \kappa_i=\frac{\cosh\,\lambda_i+\cos\,\lambda_i}{\sinh\,\lambda_i+\sin\,\lambda_i}, \tag{7}$$

where λ_i's are the roots $\lambda_1=1.8751040687$, $\lambda_2=4.6940911330,\ldots$ of the transcendental equation $1+\cos\,\lambda\cosh\,\lambda=0$, and follow the usual procedures of Galerkin's method to obtain the o.d.e set

$$\ddot{g}_i+\zeta\lambda_i^4\dot{g}_i+\lambda_i^4 g_i-\beta^2\sum_{j=1}^{n}(\alpha A_{ij}+B_{ij}+\delta_{ij})g_j+2\beta\sum_{j=1}^{n}\sum_{k=1}^{n}G_{ijk}g_j\dot{g}_k$$
$$+\sum_{j=1}^{n}\sum_{k=1}^{n}\sum_{\ell=1}^{n}[C_{ijk\ell}g_j g_k\ddot{g}_\ell+D_{ijk\ell}g_j\dot{g}_k\dot{g}_\ell+(E_{ijk\ell}-\beta^2F_{ijk\ell})g_j g_k g_\ell]=0,\quad i=1,2,\ldots,n \tag{8}$$

for the n unknown Galerkin coordinates $g_i(\tau)$ of Eq. (6). In Eq. (8), δ_{ij} is the Kronecker delta and the other coefficients are as defined in Appendix B.

Eq. (8) constitutes an approximate discretized nonlinear model for the in plane transverse vibration of the rotating beams of Fig. 1.

3. Single-dof model

A single-dof model for the i-th mode vibrations can be extracted from Eq. (8) as

$$(1 + C_{iiii}g_i^2)\ddot{g}_i + \zeta\lambda_i^4\dot{g}_i + \Omega 11_i^2 g_i + D_{iiii}g_i\dot{g}_i^2 + (E_{iiii} - \beta^2 F_{iiii})g_i^3 = 0, \tag{9}$$

where

$$\Omega 11_i = \sqrt{\lambda_i^4 - \beta^2(\alpha A_{ii} + B_{ii} + 1)} \tag{10}$$

is the i-th dimensionless linear natural frequency about the trivial equilibrium. Note that here and in what follows natural frequencies are given definite labels to avoid confusion, so that

$$\Omega JK_i, \quad \begin{cases} J: \text{ model dof} \\ K: \text{ model order of nonlinearity } (K = 1, \text{ linear; } K = 3, \text{ cubic nonlinear}) \\ i: \text{ mode number} \end{cases} \tag{11}$$

Thus, $\Omega 11_i$ reads the i-th natural frequency as obtained from a single-dof linear model. As a numerical example for Eq. (10) let one note

$$\Omega 11_1 = \sqrt{12.362363 + (1.570878\alpha + 0.193336)\beta^2}. \tag{12}$$

It should be noticed that no Coriolis term (terms with coefficients G_{ijk}) is present in Eq. (9). This is due to the fact that all the coefficients G_{ijk} vanish when $i = k$ as shown in Appendix B.

Perturbation analyses will be performed below to obtain free and forced responses of Eq. (9). But prior to that, it will be pertinent to perform a qualitative analysis on the singular (equilibrium) points of Eq. (9), their stability and bifurcations to get insight into the problem.

3.1. A qualitative analysis

It can easily be shown that Eq. (9) has three equilibrium points $\overline{g}_i$ whose stability is controlled by the characteristic roots $\rho_{1,2} = -0.5\zeta\overline{\lambda}_i^4 \mp \sqrt{(0.5\zeta\overline{\lambda}_i^4)^2 - \overline{\omega}_i^2}$ of the corresponding linearized equations, where

$$\overline{\lambda}_i^4 = \frac{\lambda_i^4}{1 + C_{iiii}\overline{g}_i^2}, \tag{13a}$$

$$\overline{\omega}_i^2 = \frac{\Omega 11_i^2 + 3(E_{iiii} - \beta^2 F_{iiii})\overline{g}_i^2}{1 + C_{iiii}\overline{g}_i^2}. \tag{13b}$$

These are the trivial equilibrium point:

$$\overline{g}_i = 0, \quad \overline{\omega}_i^2 = \Omega 11_i^2, \tag{14}$$

and the two non-trivial ones

$$\overline{g}_i = \pm\sqrt{\frac{\Omega 11_i^2}{\beta^2 F_{iiii} - E_{iiii}}}, \tag{15a}$$

$$\overline{\omega}_i^2 = \overline{\Omega} 11_i^2 = \frac{2\Omega 11_i^2(E_{iiii} - \beta^2 F_{iiii})}{C_{iiii}\Omega 11_i^2 - (E_{iiii} - \beta^2 F_{iiii})}, \tag{15b}$$

where the corresponding linear natural frequency obtained by inserting the related $\overline{g}_i$ value into Eq. (13b) is also given for each point, and $\Omega 11_j$ is as given in Eq. (10). The stability of the equilibrium points are dictated by the sign of $\overline{\omega}_i^2$ so that the point is a stable centre, node or focus depending on the value of ζ if $\overline{\omega}_i^2 > 0$, an unstable saddle if $\overline{\omega}_i^2 < 0$ and a bifurcation occurs as $\overline{\omega}_i^2$ changes the sign. Eqs. (15a) and (15b) show at a glance that as $C_{iiii} > 0$, $i = 1,2,\ldots$ (see Appendix B), the denominator of Eq. (15b) cannot change sign as long as the

numerator and the denominator of Eq. (15a) have the same sign i.e., as long as the equilibrium point of Eq. (15a) exists. Hence, the condition for a bifurcation to occur reduces for both Eqs. (14), (15a) and (15b) to $\overline{\omega}_i^2 = 0$ giving two possible bifurcation conditions. These are $\Omega 11_j = 0$ that yields

$$\beta 11_i^{\mathrm{BFC}}(\alpha) = \frac{\lambda_i^2}{\sqrt{\alpha A_{ii} + B_{ii} + 1}} \quad \text{or} \quad \alpha 11_i^{\mathrm{BFC}}(\beta) = \frac{\lambda_i^4/\beta^2 - B_{ii} - 1}{A_{ii}}, \tag{16}$$

and $E_{iiii} - \beta^2 F_{iiii} = 0$ that yields

$$\overline{\beta} 11_i^{\mathrm{BFC}} = \sqrt{\frac{E_{iiii}}{F_{iiii}}}, \tag{17}$$

where the labelling method of Eq. (11) is applied. As $A_{ii}<0$, $B_{ii}<0$, $i = 1,2,\ldots$ (see Appendix B), the bifurcation of Eq. (16) can occur in any i-th mode but only when $\alpha<-(B_{ii}+1)/A_{ii}$, a negative value. That bifurcation corresponds to the well-known buckling problem of inward-oriented rotating beams extensively treated in the literature both linearly, e.g., [19–21] and nonlinearly [11,12]. On the other hand, as $E_{iiii}>0$; $i = 1,2,\ldots$ and $F_{iiii}>0$; $i = 2,3,\ldots$ but $F_{1111}<0$ (see Appendix B), the bifurcation of Eq. (17) exists in higher modes but does not exist in the first mode. (It should be noted here that this result departs from those of Ref. [11] where a counterpart of Eq. (17) was found to apply to the first mode.) Considering now the equilibrium points and their stability; it can easily be seen that (i) the trivial equilibrium of Eq. (14) always exists. It is stable if $\beta<\beta 11_i^{\mathrm{BFC}}(\alpha)$ and unstable otherwise; (ii) the non-trivial equilibria of Eqs. (15a) and (15b) exist only in the β range between the two bifurcation values $\beta 11_i^{\mathrm{BFC}}(\alpha)$ and $\overline{\beta} 11_i^{\mathrm{BFC}}$ (where a non-existing bifurcation value should be understood as $+\infty$). They are stable if $\beta>\beta 11_i^{\mathrm{BFC}}(\alpha)$ and unstable otherwise. Hence, the existing non-trivial equilibria are all unstable if $\overline{\beta} 11_i^{\mathrm{BFC}}<\beta 11_i^{\mathrm{BFC}}(\alpha)$; (iii) it results from (i) and (ii) above that no stable equilibrium exists in the range $\beta>\max(\beta 11_i^{\mathrm{BFC}}(\alpha), \overline{\beta} 11_i^{\mathrm{BFC}})$. As $\overline{\beta} 11_1^{\mathrm{BFC}} = \infty$, this implies that a stable equilibrium is always (for any beam and at any speed) warranted at the fundamental mode, but that an inward-oriented beam with $\alpha<-(B_{ii}+1)/A_{ii}$ for which $\beta 11_i^{\mathrm{BFC}}(\alpha)\neq\infty$ will experience total collapse at higher modes for which $\overline{\beta} 11_i^{\mathrm{BFC}}\neq\infty$, $i = 2,3,\ldots$ when its speed exceeds a given β threshold.

Sample bifurcation diagrams versus dimensionless rotation speed β are given in Fig. 2 for the first two modes. An inspection of this figure with the calculated bifurcation values $\beta 11_1^{\mathrm{BFC}}(-4) = 1.4247$, $\beta 11_2^{\mathrm{BFC}}(-4) = 4.0839$, $\beta 11_1^{\mathrm{BFC}}(-1) = 2.9957$, $\beta 11_2^{\mathrm{BFC}}(-1) = 12.3779$, and $\overline{\beta} 11_2^{\mathrm{BFC}} = 8.0601$ kept in mind, gives an idea on the above described behaviour of the equilibrium points. Note for example the total collapse zones apparent in Figs. 2a_2 and b_2.

It should, however, be mentioned here that of the results obtained in this section, those concerning the behaviour of the system at a distance from the trivial equilibrium are not definitive because first, the validity of the used mathematical model is essentially restricted to the vicinity of the straight beam configuration, and second, all the nonlinear terms are truncated at the third degree, overlooking thus further possible equilibria. Only behaviours about a stable trivial equilibrium will be considered in the rest of this study.

3.2. Free vibrations

Let the i-th mode undamped free vibrations about the trivial equilibrium be examined through Eq. (9) by means of a perturbation method. To this end, put $\zeta = 0$ and $g_i \leftarrow g_i\sqrt{\varepsilon}$ (which amounts to assuming that g_i^2 shall remain at the order of ε; a small parameter) into Eq. (9) to obtain

$$\ddot{g}_i + \Omega 11_i^2 g_i + \varepsilon[C_{iiii} g_i^2 \ddot{g}_i + D_{iiii} g_i \dot{g}_i^2 + (E_{iiii} - \beta^2 F_{iiii}) g_i^3] = 0. \tag{18}$$

At that point, a brief comment on the introduced perturbation parameter ε will be in order. There are two ways of introducing such a parameter into a nonlinear differential equation. It can either be extracted from the equation itself in the form of a well-defined dimensionless function of the system parameters by means of a designed non-dimensionalization of the equation (Cole and Kevorkian [22]). Or, it can be artificially introduced into the equation (Nayfeh and Mook [23]) to serve as a "book keeping procedure" during the calculations, and then discarded by setting $\varepsilon = 1$. Although the former way has obvious advantages whenever

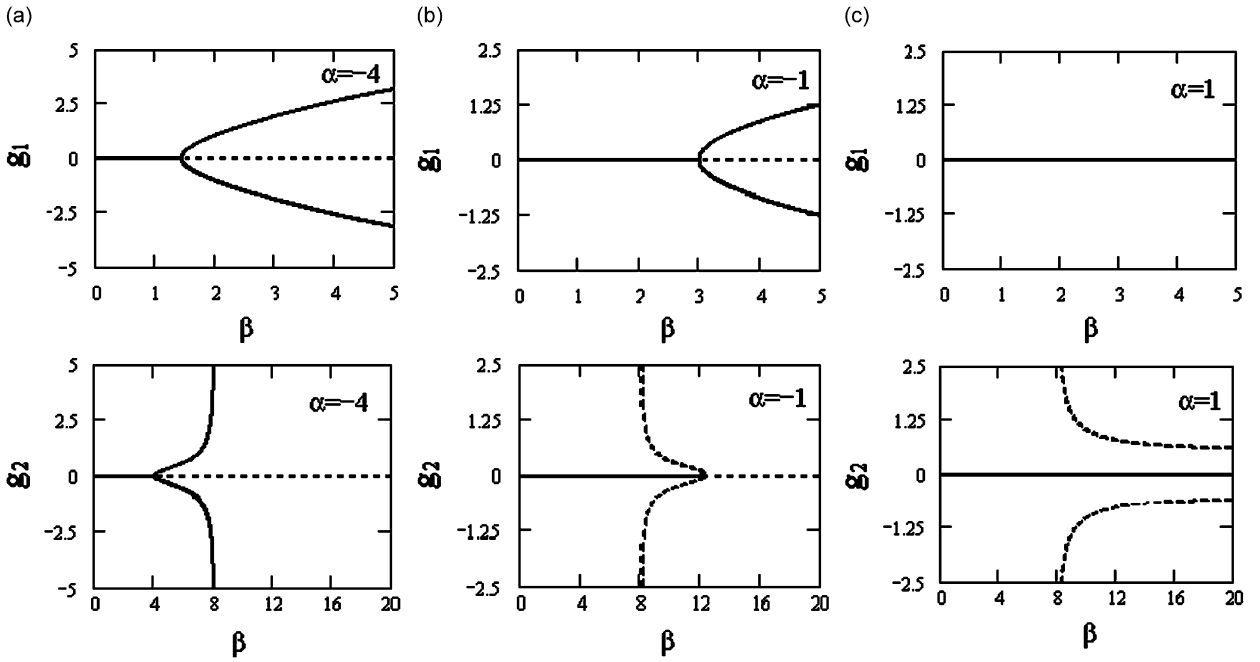

Fig. 2. Bifurcation of the equilibria with changing β: (a) $\alpha=-4$; (b) $\alpha=-1$; (c) $\alpha=1$; upper row first mode, lower row second mode (solid lines stable centers, nodes or foci, dashed lines unstable saddles).

it is applicable, the second way had to be taken in the present study where the equation is already non-dimensionalized to fit other requirements. Periodic solutions of Eq. (18) can approximately be obtained by means of LP method (see Refs. [24] or [25] for example). Assuming initial conditions $g_i(0)=G_i$, $\dot{g}_i(0)=0$ and applying the method, (Details are omitted for sake of brevity.) one obtains, up to $O(\varepsilon^2)$ terms

$$g_i(\tau)=G_i\cos\,\Omega 13_i\tau+\frac{G_i^3}{32}\left(C_{iiii}+D_{iiii}-\frac{E_{iiii}-\beta^2F_{iiii}}{\Omega 11_i^2}\right)(\cos\,\Omega 13_i\tau-\cos\,3\Omega 13_i\tau), \tag{19}$$

with the amplitude dependent i-th natural frequency $\Omega 13_i$ given, up to $O(\varepsilon^2)$ terms, as

$$\Omega 13_i=\left\{1+\frac{1}{8}\left[D_{iiii}+3\left(\frac{E_{iiii}-\beta^2F_{iiii}}{\Omega 11_i^2}-C_{iiii}\right)\right]G_i^2\right\}\Omega 11_i, \tag{20}$$

where $\Omega 11_i$ is as given in Eq. (10) and the dependence on ε is removed by setting $\varepsilon=1$. The validity of the solution is, therefore, restricted to the cases where $G_i{}^2$ is small enough. Note that Eq. (20) reduces to Eq. (10) when $G_i=0$, as it should. As a numerical example let one note

$$\Omega 13_1=\left[1+\left(\frac{3.791312+0.058151\beta^2}{\Omega 11_1^2}-0.229148\right)G_1^2\right]\Omega 11_1. \tag{21}$$

Before proceeding with the analysis, it will be in order to check the validity of the obtained solution. But recall first from Section 3.1 that its validity is already restricted to the cases where the trivial equilibrium is stable i.e., where $\beta<\beta 11_i^{\mathrm{BFC}}(\alpha)$. The solutions given by Eqs. (19) and (20) are compared in Table 1 to the numerical solutions of Eq. (18). Comparisons are presented for the first mode and for different values of the parameters α, β and amplitude G_1 throughout the period T of the related motion, where T is calculated from Eq. (21). An inspection of Table 1 shows that the performance of the LP solution is excellent for a quite high dimensionless amplitude value of $G_1=0.1$ and still acceptable for an exaggerated value of $G_1=0.5$, irrespective of the values of the parameters α and β. It is then concluded that Eqs. (19) and (20) can reliably be used to study the

Table 1
Comparison of the Lindstedt–Poincaré (LP) solutions to numerical solutions.

$\alpha = 0.5$, $\beta = 1$					$\alpha = 5$, $\beta = 10$				
τ	$G_1 = 0.1$ ($T = 1.719165$)		$G_1 = 0.5$ ($T = 1.695022$)		τ	$G_1 = 0.1$ ($T = 0.220214$)		$G_1 = 0.5$ ($T = 0.232364$)	
	g_1 (LP)	g_1 (num)	g_1 (LP)	g_1 (num)		g_1 (LP)	g_1 (num)	g_1 (LP)	g_1 (num)
0	0.100000	0.100000	0.500000	0.500000	0	0.100000	0.100000	0.500000	0.500000
0.4	0.010947	0.010947	0.052113	0.054348	0.05	0.014487	0.014487	0.130202	0.128919
0.8	−0.097672	−0.097671	−0.495085	−0.493618	0.10	−0.095936	−0.095934	−0.469940	−0.465020
1.2	−0.032301	−0.032303	−0.153255	−0.158568	0.15	−0.042210	−0.042209	−0.345264	−0.336118
1.6	0.090785	0.090782	0.479724	0.474331	0.20	0.084033	0.084029	0.360031	0.354587
T	0.100000	0.100000	0.499955	0.500000	T	0.100000	0.100000	0.499989	0.500000

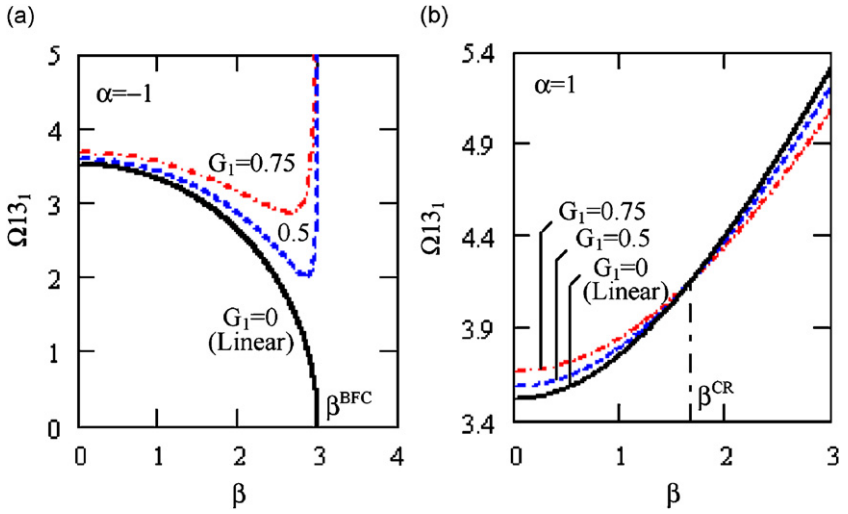

Fig. 3. Effect of the amplitude on the rotation speed dependence of the fundamental frequency: (a) an inward-oriented beam ($\alpha = -1$); (b) an outward-oriented beam ($\alpha = 1$).

behaviour of the moderately high amplitude solutions of Eq. (18), though one should yet be cautious about making deductions on those of the original Eq. (3). We will return to that question in Section 4.

Fig. 3 shows the rotation speed dependence of the fundamental frequency as obtained from Eq. (21). An inward-oriented beam with $\alpha = -1$ is considered in Fig. 3a, and an outward-oriented one with $\alpha = 1$ in Fig. 3b. Curves are given for two different values of the amplitude G_1 along with the linear frequency curves labelled $G_1 = 0$. The latter ones exhibit some well-known effects of the rotation speed on the natural frequencies. In inward-oriented beams, it may decrease the frequency until it vanishes, i.e., loss of trivial equilibrium stability (buckling) occurs at the related mode, and in outward-oriented ones it regularly increases it. Considering now the nonlinear curves, an inspection of Fig. 3a shows that the larger is the amplitude G_1 the higher is the frequency. Hence, the considered inward-oriented beam exhibits hardening behaviour. One also notes that the performance of Eq. (21) deteriorates in the vicinity of $\beta 11_1^{\mathrm{BFC}}(-1) = 2.9957$ before going totally invalid at that point. As for Fig. 3b; this figure shows that the considered outward-oriented beam displays hardening behaviour below a certain critical value β^{CR} of β but softening behaviour above it. The critical conditions can be obtained from Eq. (20) by setting the coefficient of G_i^2 to zero. This yields

$$\beta 13_i^{\mathrm{CR}}(\alpha) = \sqrt{\frac{E_{iiii} - \left(C_{iiii} - \frac{1}{3}D_{iiii}\right)\lambda_i^4}{3F_{iiii} - \left(C_{iiii} - \frac{1}{3}D_{iiii}\right)(\alpha A_{ii} + B_{ii} + 1)}} \quad \text{or} \quad \alpha 13_i^{\mathrm{CR}}(\beta) = \alpha 11_i^{\mathrm{BFC}}(\beta) - \frac{1}{A_{ii}} \frac{\frac{1}{\beta^2}E_{iiii} - F_{iiii}}{C_{iiii} - \frac{1}{3}D_{iiii}}, \tag{22}$$

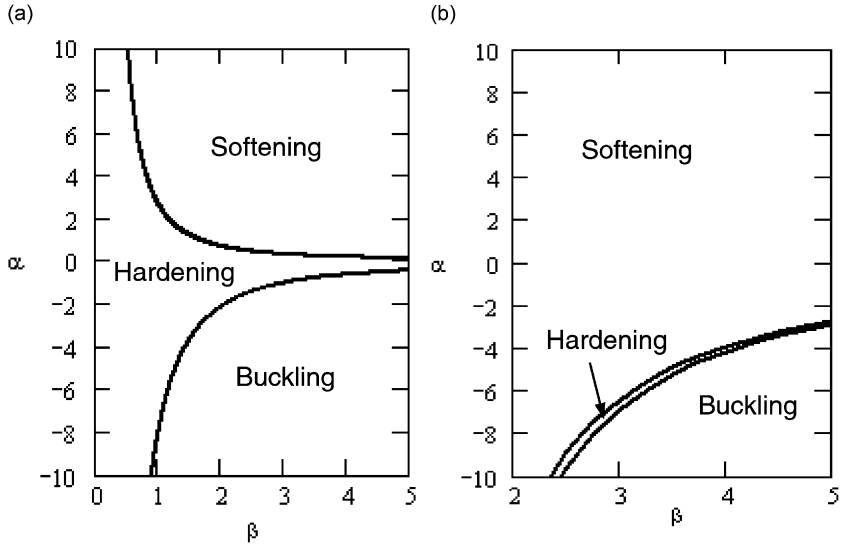

Fig. 4. Softening, hardening and buckling regions: (a) first mode; (b) second mode.

where again the labelling method of Eq. (11) is applied. The beam exhibits hardening behaviour in the i-th mode if $\alpha<\alpha 13_i^{CR}(\beta)$ and softening behaviour if $\alpha>\alpha 13_i^{CR}(\beta)$. The corresponding regions of a $\alpha-\beta$ parameter plane are shown in Figs. 4a and b for the first two modes together with the buckling regions defined in Eq. (16), where the present solution loses its validity. An inspection of Fig. 4a shows that in the first mode, an inward-oriented ($\alpha<0$) beam always behaves as a hardening spring unless it is buckled. But that an outward-oriented ($\alpha>0$) beam may show hardening or softening behaviour depending on the values of α and β, so that for a given value of the dimensionless hub radius α it may behave as a hardening spring at low speeds but switch to a softening one at high speeds. On the other hand, Fig. 4b shows that in the second mode, an inward-oriented ($\alpha<0$) beam generally behaves as a softening spring, except in a narrow parameter band surrounding the buckling region, and that an outward-oriented ($\alpha>0$) one always behaves as a softening spring.

The most noteworthy result of the present analysis is that a speed change may cause a passage from hardening to softening behaviour, i.e., a qualitative change in the dynamic character of a given rotating beam. It should be noted that the results obtained in this section differ from those of Ref. [15] where it was stated that an outward-oriented rotating beam would always exhibit hardening behaviour in the first mode and softening behaviour in higher modes, and that the first mode would suffer loss of stability at low (even zero) amplitudes when the rotation speed is high.

3.3. Response to harmonic excitation

Let now the response to harmonic excitation of the single mode model be examined. Returning to Eq. (18), putting $g_i \leftarrow g_i\sqrt{\varepsilon}$, introducing a modal damping with coefficient $\mu_i=\varepsilon\zeta\lambda_i^4/2$ and a harmonic modal forcing in the form $\sqrt{\varepsilon}F_i\cos\overline{\Omega}\tau$, where the damping is scaled so as to take effect at the same order as the nonlinearities but the forcing at that of the linear terms, one has

$$\ddot{g}_i+\Omega 11_i^2 g_i+\varepsilon[C_{iiii}g_i^2\ddot{g}_i+2\mu_i\dot{g}_i+D_{iiii}g_i\dot{g}_i^2+(E_{iiii}-\beta^2F_{iiii})g_i^3]=F_i\cos\overline{\Omega}t. \tag{23}$$

The main, super-harmonic and sub-harmonic resonances of this model are studied below, via again the LP method.

Main resonance: To study the system behaviour at the main resonance, assume

$$\overline{\Omega}=\Omega 11_i(1+\sigma\varepsilon),\quad F_i=\varepsilon f_i, \tag{24}$$

where σ is a detuning parameter and the forcing is now rescaled to take effect at the same order as the damping and the nonlinearities. This scaling, that essentially amounts to assuming that no strong forcing is necessary to

get characteristic resonant behaviour of the system, is known to be appropriate in the main resonance behaviour analysis of the forced Duffing oscillator, a paradigm for systems with cubic nonlinearities, will prove to be equally valid here. (This rescaling will not be applied in the analysis of the sub and super-harmonic resonances where a strong forcing proves to be necessary to obtain characteristic resonance behaviour of the system, as is the case in the analysis of Duffing's equation.) Applying now the method (details omitted) one obtains the steady-state response, up to $O(\varepsilon)$ terms, as

$$g_i(\tau) = G_i \cos(\overline{\Omega}\tau - \theta_i), \tag{25}$$

where the amplitude G_i, the phase angle θ_i and the detuning parameter σ are interrelated through

$$\sigma = \frac{\Omega 13_i}{\Omega 11_i} - 1 \pm \frac{1}{\Omega 11_i^2}\sqrt{\frac{F_i^2}{4G_i^2} - \mu_i^2 \Omega 11_i^2}, \tag{26}$$

$$\theta_i = \tan^{-1}\frac{\mu_i}{\Omega 13_i - (1+\sigma)\Omega 11_i}, \tag{27}$$

where $\Omega 11_i$ and $\Omega 13_i$ must be substituted from Eqs. (10) and (20), respectively, and dependence on ε is again removed by setting $\varepsilon = 1$.

Fig. 5 shows the variation of the amplitude G_1 and phase angle θ_1 of the first mode with the detuning parameter σ, as obtained from Eqs. (26) and (27). Curves are presented for $\alpha = 1$, $F_1 = 0.0025$, $\mu_1 = 0.001$, and three different values of β corresponding to different regions of Fig. 4a. Namely, $\beta = 1$ corresponding to the hardening region, $\beta = 2$ to the softening one, and $\beta^{CR} = 1.664123$ to the boundary separating the two regions. The critical value of β is calculated from Eq. (22) with $\alpha = 1$. An inspection of Fig. 5 (and others not reproduced here) shows that (i) the inclinations of the resonance curves (rightward for a hardening system and leftward for a softening one) are in accordance with Fig. 4a; (ii) jump phenomena may accompany a frequency change in the forcing, provided that the force amplitude is sufficiently high, the damping is sufficiently low and the rotation speed is sufficiently far from its critical value; (iii) in an outward-oriented beam, the lower is the rotation speed of the beam the higher is its resonance peak. Thus, a low speed main resonance is more dangerous than a high speed one. This can also readily be deduced from Eq. (26) whose validity requires the term under the radical to be non-negative, i.e.,

$$G_i \leqslant \frac{F_i}{2\mu_i \Omega 11_i}. \tag{28}$$

Thus, the peak (that corresponds to the equal sign in Eq. (28)) of a resonance curve of an i-th mode is inversely proportional to the natural frequency $\Omega 11_i$, which is known to regularly increase with the rotation speed in outward-oriented beams. (No such generalization is possible for inward-oriented ones whose natural frequencies may increase or decrease with the rotation speed.)

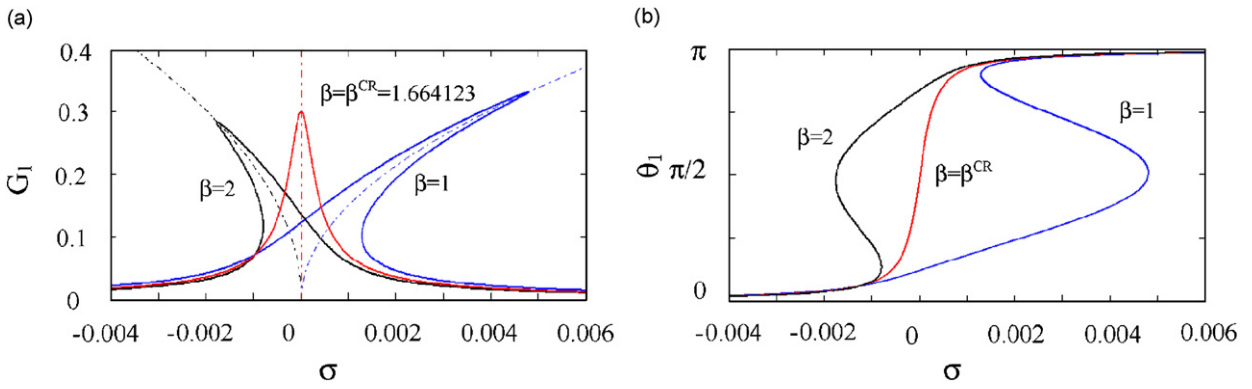

Fig. 5. Main resonance of the first mode, forcing frequency changes: (a) amplitudes; (b) phases ($\alpha = 1$, $F_1 = 0.0025$, $\mu_1 = 0.001$).

The resonance curves of Fig. 5 are obtained in the ordinary way of varying the forcing frequency through a natural frequency while keeping all the other parameters fixed. But, as its natural frequencies depend on the rotation speed, a rotating beam can also be driven through resonance by simply changing its rotation speed while keeping the forcing frequency constant (This may be the case when the excitation is due to an external cause.). Then, if the resonance is to occur at a speed β_{res}, the detuning parameter will read

$$\sigma(\beta) = \frac{1}{\varepsilon}\left(\frac{\Omega 11_i(\alpha, \beta_{\text{res}})}{\Omega 11_i(\alpha, \beta)} - 1\right), \tag{29}$$

where now $\varepsilon = 1$. Fig. 6 shows some resonance curves corresponding to different β_{res} values for the first mode of an outward-oriented beam with parameter values $\alpha = 1$ ($\beta^{\text{CR}} = 1.664123$), $F_1 = 0.015$, $\mu_1 = 0.004$, as obtained by inserting Eq. (29) into Eq. (26). Interpreting Fig. 6 one should note that, in contrast with Fig. 5, the detuning parameter decreases here from left to right so as $\sigma = 0$ at $\beta = \beta_{\text{res}}$. The inclinations of hardening and softening resonance curves are therefore reversed. Upon inspection of Fig. 6 one notes that: (i) the shape of the resonance curve closely depends on the β_{res} value at which resonance occurs; (ii) in accordance with Fig. 5, the curve is of hardening nature when $\beta_{\text{res}} < \beta^{\text{CR}}$, of softening nature when $\beta_{\text{res}} > \beta^{\text{CR}}$, and of linear nature when $\beta_{\text{res}} = \beta^{\text{CR}}$. Jump phenomena may, therefore, accompany a speed change if the resonant speed is sufficiently far from the critical speed; (iii) a low speed resonance (such as those occurring at $\beta_{\text{res}} = 0.25$ and $\beta_{\text{res}} = 0.5$ for example) is especially dangerous as it can give rise to very high amplitudes over the whole speed range below the resonant speed. (This is due to the almost stationary behaviour of the natural frequencies against rotation speed at low speeds. See Fig. 3.)

As Eq. (23) describes a system with cubic nonlinearities (3x) super-harmonic and (1/3) sub-harmonic resonances are also expected to occur. These are studied below.

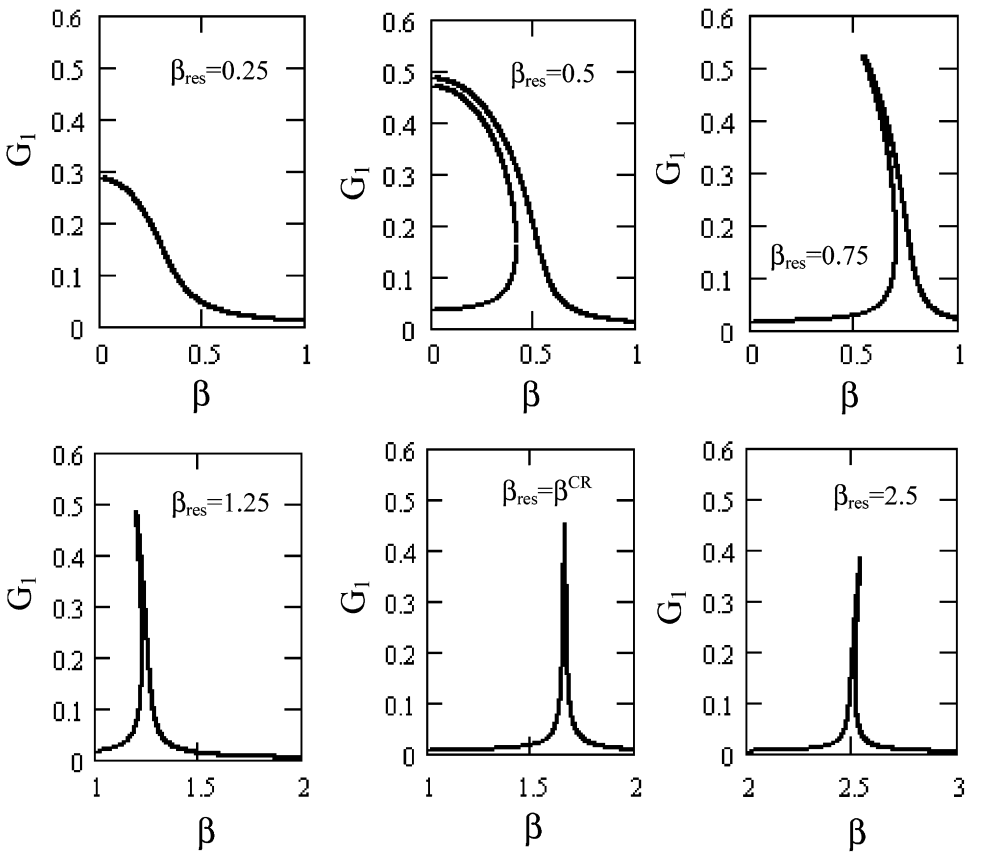

Fig. 6. Main resonance of the first mode, forcing frequency kept constant, rotation speed changes, each graph corresponds to a different resonant speed β_{res} ($\alpha = 1$, $F_1 = 0.015$, $\mu_1 = 0.004$).

Super-harmonic resonance: To study the (3x) super-harmonic resonances, assume

$$\overline{\Omega} = \frac{\Omega 11_i}{3}(1+\sigma\varepsilon), \tag{30}$$

return to Eq. (23), and apply the LP method to obtain the steady-state solution

$$g_i(\tau) = \frac{9F_i}{8\Omega 11_i^2}\cos\overline{\Omega}\tau + G_i\cos(3\overline{\Omega}\tau - \theta_i) + O(\varepsilon), \tag{31}$$

where the relations

$$\sigma = \frac{\Omega 13_i}{\Omega 11_i} - 1 + \left(\frac{3F_i}{16\Omega 11_i^2}\right)^2\left(D_{iiii} + \frac{27(E_{iiii}-\beta^2 F_{iiii})}{\Omega 11_i^2} - 11C_{iiii}\right) \pm \sqrt{\left[\frac{3}{G_i}\left(\frac{3F_i}{16\Omega 11_i^2}\right)^3\left(C_{iiii}+D_{iiii}-\frac{9(E_{iiii}-\beta^2F_{iiii})}{\Omega 11_i^2}\right)\right]^2 - \frac{\mu_i^2}{\Omega 11_i^2}} \tag{32}$$

and

$$\theta_i = \tan^{-1}\frac{\mu_i}{\Omega 13_i + \left[\left(\frac{3F_i}{16\Omega 11_i^2}\right)^2\left(D_{iiii} + 27\frac{E_{iiii}-\beta^2F_{iiii}}{\Omega 11_i^2} - 11C_{iiii}\right) - (1+\sigma)\right]\Omega 11_i} \tag{33}$$

hold true. Examples of super-harmonic resonance curves of the first mode, corresponding to parameter values $\alpha = 1$, $F_1 = 2.5$, $\mu_1 = 0.001$, and three different values of β corresponding to different regions of Fig. 4 are shown in Fig. 7. An inspection of this figure shows that the zones of Fig. 4 are still valid for super-harmonic resonances and that jump phenomena may again accompany a change in the forcing frequency. As was done in Eq. (28), the peak amplitude values can be deduced from the non-negativity condition of the term under the radical in Eq. (32);

$$G_i \leqslant \left|\frac{3}{\mu_i\Omega 11_i^5}\left(\frac{3F_i}{16}\right)^3\left(C_{iiii}+D_{iiii}-\frac{9(E_{iiii}-\beta^2F_{iiii})}{\Omega 11_i^2}\right)\right|. \tag{34}$$

Fig. 8 shows the rotation speed dependence of the peak amplitudes $G_{1\max}$ and $G_{2\max}$ of the first two modes of an outward-oriented beam as calculated from Eq. (34) with equal sign, for parameter values $\alpha = 1$, $F_1 = 2.5$, $\mu_1 = 0.001$. Note from Fig. 8a that, in contrast with the main resonance, that dependence is not uniform in all modes now. As an interesting detail let one note the vanishing of $G_{1\max}$ (i.e., the impossibility of super-harmonic resonance in the first mode) at a certain value of β, which can be shown to be given by $\beta(\alpha) = \sqrt{7.668046/11.89097\alpha - 0.092511}$.

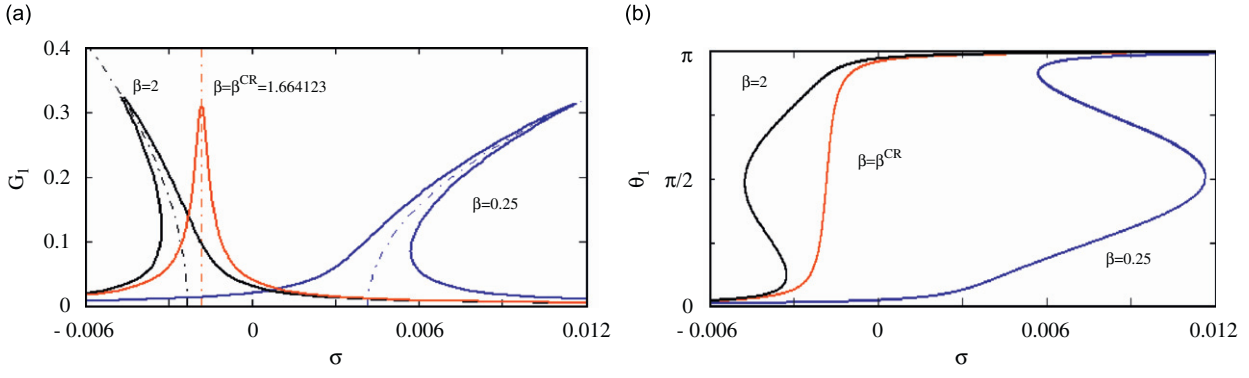

Fig. 7. Super-harmonic resonance of the first mode: (a) amplitudes; (b) phases ($\alpha = 1$, $F_1 = 2.5$, $\mu_1 = 0.001$).

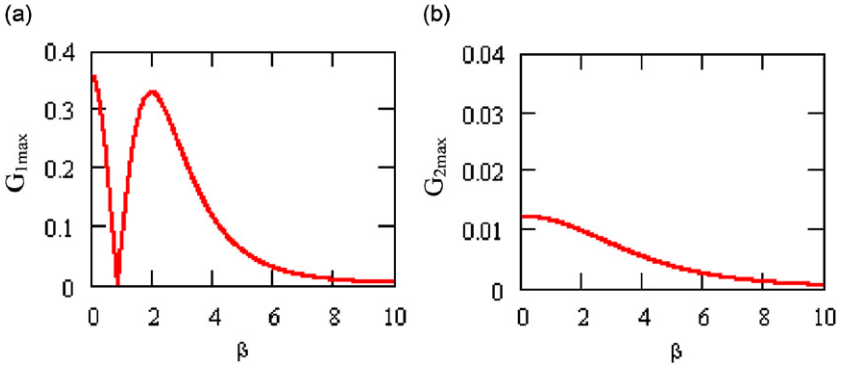

Fig. 8. Rotation speed dependence of the peak amplitudes in super-harmonic resonance: (a) first; (b) second mode ($\alpha = 1$, $F_1 = 2.5$, $\mu_1 = 0.001$).

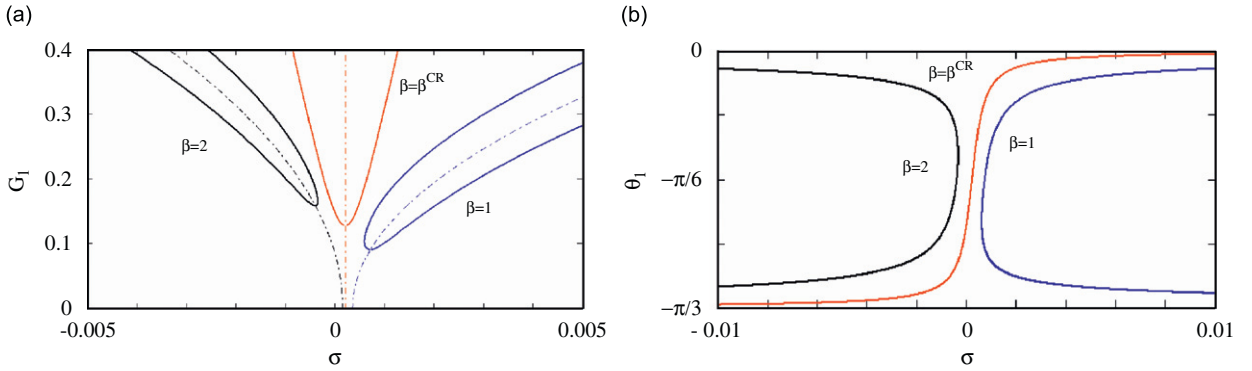

Fig. 9. Sub-harmonic resonance of the first mode: (a) amplitudes; (b) phases ($\alpha = 1 \rightarrow \beta^{CR} = 1.664123$, $F_1 = 2.5$, $\mu_1 = 0.0015$).

Sub-harmonic resonance: To study the (1/3) sub-harmonic resonances, substitute

$$\overline{\Omega} = 3\Omega 11_i(1 + \sigma\varepsilon) \tag{35}$$

into Eq. (23), apply the LP method and obtain

$$g_i(\tau) = -\frac{F_i}{8\Omega 11_i^2}\cos\,\overline{\Omega}\tau + G_i\,\cos\left(\frac{1}{3}\overline{\Omega}\tau + \theta_i\right) + O(\varepsilon) \tag{36}$$

with

$$\sigma = 1 - \frac{\Omega 13_i}{\Omega 11_i} + \left(\frac{F_i}{16\Omega 11_i^2}\right)^2\left(9D_{iiii} + \frac{3(E_{iiii} - \beta^2 F_{iiii})}{\Omega 11_i^2} - 19C_{iiii}\right) \pm \sqrt{\left(\frac{F_i G_i}{64\Omega 11_i^2}\right)^2\left(11C_{iiii} - 5D_{iiii} - \frac{3(E_{iiii} - \beta^2 F_{iiii})}{\Omega 11_i^2}\right)^2 - \frac{\mu_i^2}{\Omega 11_i^2}} \tag{37}$$

and

$$\theta_i = \frac{1}{3}\tan^{-1}\frac{-\mu_i}{\Omega 13_i - \left[\left(9D_{iiii} + \frac{3(E_{iiii} - \beta^2 F_{iiii})}{\Omega 11_i^2} - 19C_{iiii}\right)\left(\frac{F_i}{16\Omega 11_i^2}\right)^2 + (1 - \sigma)\right]\Omega 11_i}. \tag{38}$$

Examples of resonance curves are given for the first mode in Fig. 9. As can be seen in this figure (i) the hardening and softening regions of Fig. 4 are valid for sub-harmonic resonances too; (ii) in contrast with the main and super-harmonic resonances, no jump phenomenon is encountered in sub-harmonic ones; (iii) resonance curves have unique shapes with minima instead of maxima. These minima can be calculated from Eq. (37), which yields

$$G_i \geqslant \frac{64\mu_i \Omega 11_i^3}{|(11C_{iiii} - 5D_{iiii})\Omega 11_i^2 - 3(E_{iiii} - \beta^2 F_{iiii})|F_i}. \tag{39}$$

Although not elaborated here, it should be clear that both sub-harmonic and super-harmonic resonances and super-harmonic jump phenomena can be encountered during a speed change, in the same way as in the main resonance.

Let one also note that under some circumstances harmonic excitation may cause a rotating beam to undergo chaotic vibrations as was shown in Ref. [17] through a two-dof model and in Refs. [14,18] through single-dof ones. That problem is left beyond the scope of this study.

4. Two-dof model

In order to check and refine the results obtained above through a single-dof model, the undamped free vibrations of a two-dof model taken from Eq. (8) will be considered in this section. Thus consider

$$\begin{aligned}\Phi_i(g_i, g_j) = {} & [1 + C_{iiii}g_i^2 + (C_{iiji} + C_{ijii})g_i g_j + C_{ijji}g_j^2]\ddot{g}_i + [C_{iiij}g_i^2 + (C_{iijj} + C_{ijij})g_i g_j + C_{ijjj}g_j^2]\ddot{g}_j \\ & + \Omega 11_i^2 g_i - \Omega_{ij}^2 g_j + 2\beta(G_{iij}g_i + G_{ijj}g_j)\dot{g}_j + (D_{iiii}g_i + D_{ijii}g_j)\dot{g}_i^2 + 2(D_{iiij}g_i + D_{ijij}g_j)\dot{g}_i\dot{g}_j \\ & + (D_{iijj}g_i + D_{ijjj}g_j)\dot{g}_j^2 + (E_{iiii} - \beta^2 F_{iiii})g_i^3 + (\overline{E}_{iiij} - \beta^2\overline{F}_{iiij})g_i^2 g_j + (\overline{E}_{iijj} - \beta^2\overline{F}_{iijj})g_i g_j^2 \\ & + (E_{ijjj} - \beta^2 F_{ijjj})g_j^3 = 0, \quad i,j = k,\ell;\ j \neq i,\end{aligned} \tag{40}$$

where $\Omega 11_i$ is as given in Eq. (10), use is made of the previously discussed property $G_{iji} = 0$ (See Appendix B), of the equalities $D_{iiij} = D_{iiji}$, $D_{ijij} = D_{ijji}$ that directly follow from the definition Eq. (B.5) of $D_{ijk\ell}$, and of the definitions

$$\overline{E}_{iiij} = E_{iiij} + E_{iiji} + E_{ijii}, \quad \overline{F}_{iiij} = F_{iiij} + F_{iiji} + F_{ijii}, \tag{41}$$

$$\overline{E}_{iijj} = E_{iijj} + E_{ijij} + E_{ijji}, \quad \overline{F}_{iijj} = F_{iijj} + F_{ijij} + F_{ijji},$$

$$\Omega_{ij} = \beta\sqrt{(\alpha A_{ij} + B_{ij})}, \tag{42}$$

where $\Omega_{ji} = \Omega_{ij}$ due to the symmetry of the coefficients A_{ij} and B_{ij} (see Appendix B). Eq. (40) describes an approximate two-dof nonlinear model for the coupled k-th and ℓ-th mode vibrations of the rotating beam of Fig. 1. That equation contains, along with a number of nonlinear coupling terms, a linear coupling whose coefficient is given in Eq. (42). That coupling is due to the rotation of the beam and vanishes when $\beta = 0$, as could be expected in view of the fact that the stationary beam problem is already linearly decoupled during discretization by means of the eigenfunctions of a linear stationary beam. It will prove to be convenient to remove that residual linear coupling before proceeding. Hence, consider the linear part of Eq. (40)

$$\ddot{g}_i + \Omega 11_i^2 g_i - \Omega_{ij}^2 g_j = 0, \quad i,j = k,\ell;\ j \neq i, \tag{43}$$

perform its eigen-analysis to obtain the i-th natural frequency

$$\Omega 21_i = \frac{1}{\sqrt{2}}\sqrt{(\Omega 11_i^2 + \Omega 11_j^2) + \mathrm{sgn}(i-j)\sqrt{(\Omega 11_i^2 - \Omega 11_j^2)^2 + 4\Omega_{ij}^4}} \tag{44}$$

and the corresponding normalized mode vector

$$u^{(i)} = \{u_i^{(i)} \;\; u_j^{(i)}\}^{\mathrm{T}} = \gamma_i \left\{ 1 \;\; \frac{\Omega 11_i^2 - \Omega 11_j^2 - \mathrm{sgn}(i-j)\sqrt{(\Omega 11_i^2 - \Omega 11_j^2)^2 + 4\Omega_{ij}^4}}{2\Omega_{ij}^2} \right\}^{\mathrm{T}} \tag{45}$$

with

$$\gamma_i = \frac{2\Omega_{ij}^2}{\sqrt{4\Omega_{ij}^4 + [\Omega 11_i^2 - \Omega 11_j^2 - \mathrm{sgn}(i-j)\sqrt{(\Omega 11_i^2 - \Omega 11_j^2)^2 + 4\Omega_{ij}^4}]^2}}, \tag{46}$$

where $\Omega 11_i$ and $\Omega 21_j$ must be substituted from Eq. (10) and the sign function is introduced to keep the expressions valid for both the lowest ($i<j$) and the highest ($i>j$) of the coupling modes. Then, project Eqs. (40) onto the linear modal space. To this end substitute the modal decomposition

$$g_i = \eta_i u_i^{(i)} + \eta_j u_i^{(j)} \tag{47}$$

into Eq. (40) that, as a result, reads $\Phi_i(\eta_i, \eta_j) = 0$, and write

$$u_i^{(i)} \Phi_i(\eta_i, \eta_j) + u_j^{(i)} \Phi_j(\eta_i, \eta_j) = 0, \quad i,j = k,\ell; \;\; i \neq j \tag{48}$$

to obtain

$$\begin{aligned} \ddot{\eta}_i + \Omega 21_i^2 \eta_i = & -\varepsilon\{(c_{iiii}\eta_i^2 + c_{iiji}\eta_i\eta_j + c_{ijji}\eta_j^2)\ddot{\eta}_i + (c_{iiij}\eta_i^2 + c_{iijj}\eta_i\eta_j + c_{ijjj}\eta_j^2)\ddot{\eta}_j + (d_{iiii}\eta_i + d_{ijii}\eta_j)\dot{\eta}_i^2 \\ & + 2(d_{iiij}\eta_i + d_{ijij}\eta_j)\dot{\eta}_i\dot{\eta}_j + (d_{iijj}\eta_i + d_{ijjj}\eta_j)\dot{\eta}_j^2 + 2\beta[(g_{iii}\eta_i + g_{iji}\eta_j)\dot{\eta}_i + (g_{iij}\eta_i + g_{ijj}\eta_j)\dot{\eta}_j] \\ & + (e_{iiii} - \beta^2 f_{iiii})\eta_i^3 + (e_{iiij} - \beta^2 f_{iiij})\eta_i^2\eta_j \\ & + (e_{iijj} - \beta^2 f_{iijj})\eta_i\eta_j^2 + (e_{ijjj} - \beta^2 f_{ijjj})\eta_j^3\}, \quad i,j = k,\ell; \;\; i \neq j, \end{aligned} \tag{49}$$

where $\varepsilon = 1$ is a provisionally introduced parameter to label the nonlinear terms. Now, assume initial conditions $\eta_i(0) = A_i$, $\dot{\eta}_i(0) = 0$, $i = k,\ell$, discard any probability of internal resonance that can be shown to occur when $\Omega 21_j \cong p \cdot \Omega 21_i$ with $p = \frac{1}{2}, \frac{1}{3}$, 1, 2, or 3 and apply the multiple scales method (details omitted here, see Ref. [23] for the method) to obtain the solutions $\eta_i(\tau) = A_i \cos \Omega 23_i \tau + O(\varepsilon)$, $i = k, \ell$ where the natural frequency $\Omega 23_i$ is given up to $O(\varepsilon^2)$ terms as

$$\Omega 23_i = \left\{ 1 + \frac{1}{8}\left[d_{iiii} + 3\left(\frac{e_{iiii} - \beta^2 f_{iiii}}{\Omega 21_i^2} - c_{iiii} \right) \right] A_i^2 + \frac{1}{4}\left[\frac{e_{iijj} - \beta^2 f_{iijj} + (d_{iijj} - c_{iijj})\Omega 21_j^2}{\Omega 21_i^2} - c_{ijji} \right] A_j^2 \right\} \Omega 21_i,$$
$$i,j = k,\ell; \;\; i \neq j, \tag{50}$$

where $\Omega 21_i$ and $\Omega 21_j$ must be substituted from Eq. (44) and the other coefficients are as defined in Appendix C. Eq. (50) reduces, as it should, to the two-dof linear frequency of Eq. (44) when both A_i and A_j vanish, and to the single-dof nonlinear frequency of Eq. (20) when coupling is ignored. This equation that accounts for the contribution of the j-th mode on the i-th natural frequency obviously constitutes a refined counterpart of Eq. (20). Note however that the effect of the Coriolis terms with coefficients g_{ijk} does not appear at that level of approximation. The first two frequencies calculated from Eq. (50) with $k = 1$, $\ell = 2$ (i.e., coupling of the first two modes are considered), are compared on Table 2 to those calculated from Eq. (20) for different α, β and modal amplitude values. The values appearing on the first column of the table refer to the amplitude of the mode whose frequency is calculated, i.e., to A_i for a column of $\Omega J3_i$'s. The other modal amplitude is set to zero in each case. Reliable results obtained by Naguleswaran [5,6] via a Frobenius series analysis of the linear part of Eq. (3) (Hence corresponding to $A_1 = A_2 = 0$.) are also shown on the table. Results for $\alpha \geqslant 0$ are taken from Table 3, cl–fr boundary conditions of Ref. [5], while those for $\alpha < 0$ from Table 3, cl–fr boundary conditions of Ref. [6], where they were given for out-of-plane vibrations. The in-plane frequencies needed here are obtained by using the relation [5] $\Omega_{\mathrm{in}}^2 = \Omega_{\mathrm{out}}^2 - \beta^2$.

A triple comparison of the linear results suggests that (i) Eq. (50) constitutes in fact a refinement over Eq. (20) with respect to the fundamental frequency calculations but that its contribution is dubious with

Table 2
Comparison of the nonlinear frequencies from single-dof and two-dof models.

A_1 or A_2	Source	$\beta=1,\ \alpha=-1$		$\beta=1,\ \alpha=0$		$\beta=1,\ \alpha=1$		$\beta=5,\ \alpha=1$	
		$\Omega J3_1$	$\Omega J3_2$	$\Omega J3_1$	$\Omega J3_2$	$\Omega J3_1$	$\Omega J3_2$	$\Omega J3_1$	$\Omega J3_2$
0	Eq. (20) ($J=1$)	3.314336	21.962466	3.543402	22.158453	3.758534	22.352722	7.514501	28.959506
	Eq. (50) ($J=2$)	3.314314	21.962469	3.543264	22.158475	3.758198	22.352779	7.449006	28.976422
	Refs. [5,6]	3.3143	21.9624	3.5432	22.1584	3.7580	22.3526	7.4115	28.9238
0.05	Eq. (20) ($J=1$)	3.315341	20.543648	3.544088	20.724469	3.758941	20.903726	7.511941	26.969565
	Eq. (50) ($J=2$)	3.315304	20.543406	3.543915	20.723858	3.758554	20.902767	7.446231	26.967548
0.1	Eq. (20) ($J=1$)	3.318356	16.287193	3.546146	16.422515	3.760163	16.556737	7.504262	20.999742
	Eq. (50) ($J=2$)	3.318273	16.286218	3.545868	16.420007	3.759622	16.552730	7.437906	20.940925
0.25	Eq. (20) ($J=1$)	3.339460	Unstable	3.560553	Unstable	3.768717	Unstable	7.450505	Unstable
	Eq. (50) ($J=2$)	3.339063	Unstable	3.559539	Unstable	3.767101	Unstable	7.379633	Unstable
0.5	Eq. (20) ($J=1$)	3.414832	Unstable	3.612005	Unstable	3.799267	Unstable	7.258517	Unstable
	Eq. (50) ($J=2$)	3.413310	Unstable	3.608364	Unstable	3.793811	Unstable	7.171514	Unstable

Amplitude of the other mode set to zero in 2 dof calculations.

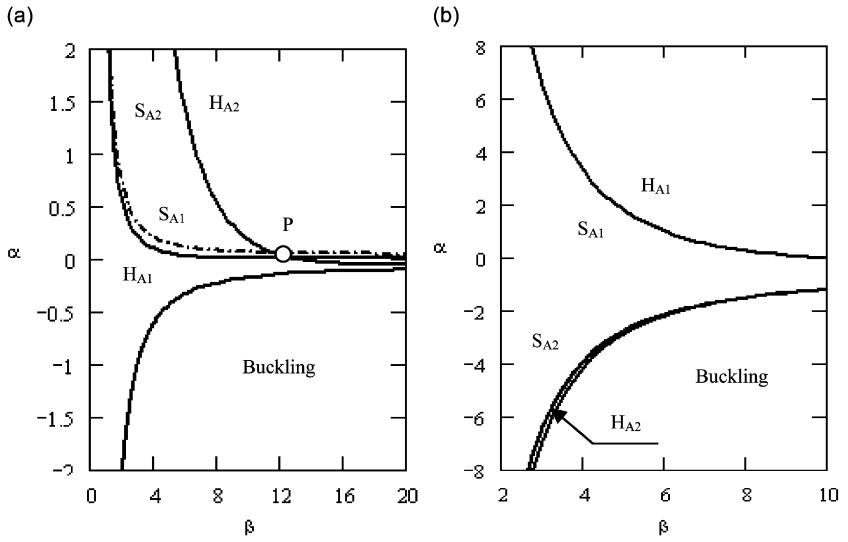

Fig. 10. Softening, hardening and buckling regions: (a) first mode; (b) second mode (S_{Ai}: softening, H_{Ai}: hardening w.r.t. i-th modal amplitude; -.-: result from single-dof model).

respect to the second frequency, for a reliable analysis of which, consideration of at least the two intercepting modes seems to be necessary; (ii) the convergence of the two-dof model is satisfactory for medium values (such as $\beta=1$) of the parameter β, but wanting at high values (such as $\beta=5$) of it. The nonlinear results on that table also confirm that conclusion. Let one note that a similar trend was also observed for the parameter α. Combining now these results with those deduced from Table 1, Section 3.1 one may conclude that Eq. (50) can reliably be used to predict, at least, the fundamental mode behaviour of the solutions of Eq. (3), provided that the amplitudes and the parameters α and β are not too large.

Eq. (50) shows that $\alpha-\beta$ parameter combinations may arise for which the coefficients of A_i^2 or A_j^2 vanish. Those combinations that obviously correspond to the boundaries of hardening and softening regions of the i-th mode with respect to the i-th and j-th modal amplitudes are calculated for $i=1, j=2$ and presented in Fig. 10, where the buckling regions mentioned in Section 3.1 are also shown. (It turns out that the buckling boundaries, i.e., bifurcation points $\beta 21_i^{BFC}(\alpha)$ correspond now to the vanishing conditions of the frequencies of Eq. (44).) This figure, which is a refinement to Fig. 4 (see the hardening–softening boundary of Fig. 4a reproduced in Fig. 10a), shows that the parameter plane is divided for each mode into different regions where hardening or softening with respect to either of the modal amplitudes, prevails. (At the point P; $\alpha=0.009$, $\beta=12.670$ of Fig. 10a the fundamental frequency gets independent of both amplitudes.) If one considers the total portrait of the beam by superimposing the Figs. 10a and b, one concludes that a given beam may be guided through a multitude of variety of dynamic characters by simply changing its rotation speed.

In the softening parameter zones where a frequency decreases with increasing amplitude, a critical combination of modal amplitudes may occur where the frequency vanishes; i.e., the related mode vibrations lose their stability. Fig. 11 shows the loci of such critical combinations for the first (Fig. 11a) and second (Fig. 11b) modes for different values of the parameters α and β corresponding to different regions of Fig. 10. Only a quarter of the diagrams are shown due to double symmetry. As can easily be deduced from the structure of Eq. (50), these loci always form conic sections; specifically ellipses when the considered mode is softening with respect to both modal amplitudes and hyperbolas when it is hardening with respect to an amplitude and softening with respect to the other. The cells labelled "unstable" in Table 2 fall to the unstable side of the critical loci relative to the given $\alpha-\beta$ pair. (Compare the column $\alpha=1$, $\beta=1$ of the table to Fig. 11.)

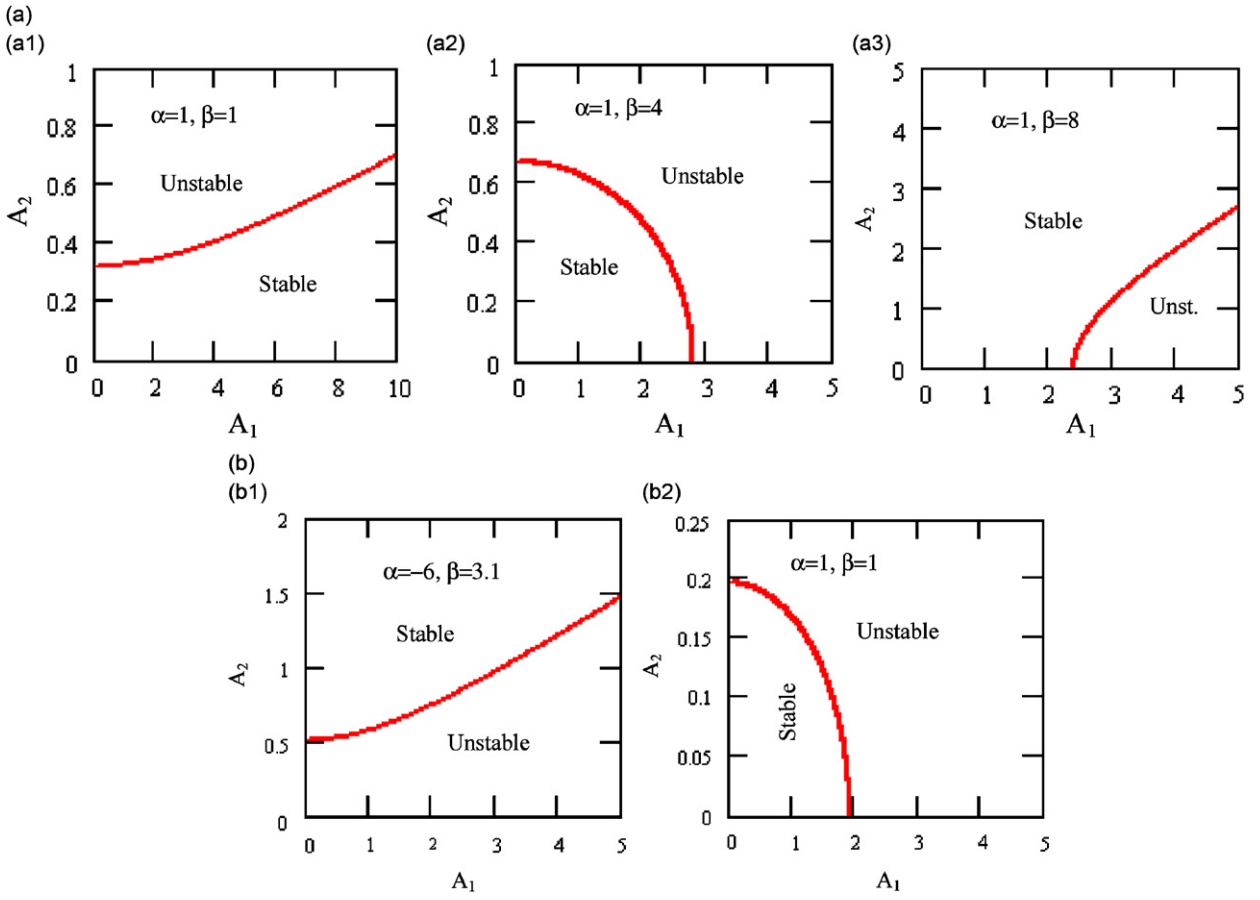

Fig. 11. Critical amplitude combinations for (a) first and (b) second mode.

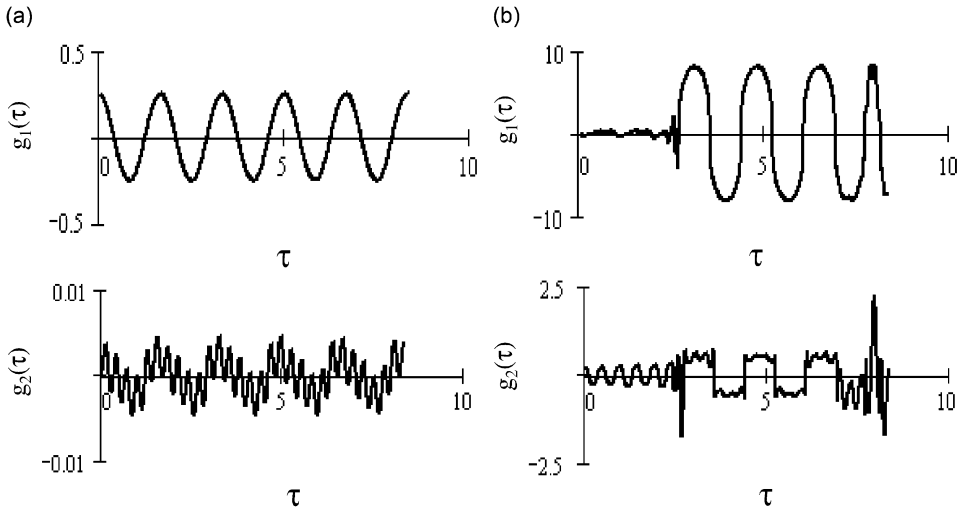

Fig. 12. Numerical solutions of Eq. (40) for $\alpha = 1$, $\beta = 1$: (a) $g_1(0) = 0.25$, $g_2(0) = 0$, $\dot{g}_1(0) = \dot{g}_2(0) = 0$; (b) $g_1(0) = 0$, $g_2(0) = 0.25$, $\dot{g}_1(0) = \dot{g}_2(0) = 0$.

Finally, two numerical solution examples of Eq. (40), both corresponding to the same parameter values $\alpha = 1$, $\beta = 1$, but to different initial conditions, are presented in Figs. 12a and b. The initial conditions of Fig. 12a [$g_1(0) = 0.25$, $g_2(0) = 0 \rightarrow A_1 = 0.249999$, $A_2 = 0.000571$] correspond to a stable modal amplitude combination for both modes according to Fig. 11, while those of Fig. 12b ($g_1(0) = 0$, $g_2(0) = 0.25 \rightarrow A_1 = 0.000571$, $A_2 = -0.249999$) corresponding to an unstable combination for the second mode. These figures verify the above analysis results and give an idea on stable and unstable motions. (Although the behaviour of the solutions of Eq. (40) has some interesting features that deserve a separate theoretical analysis, this problem is not considered here.)

5. Conclusions

The in plane nonlinear vibrations of a rotating beam are studied via single- and two-degree-of-freedom models obtained through Galerkin discretization. The beam is assumed to have nonlinear curvature and all nonlinearities of both geometric and dynamic origin are maintained in the model up to cubic terms. Bifurcation of the equilibria, amplitude dependent natural frequency calculation and frequency response problems are considered. All the formulations and results are given in a general form but the interest is focused on the behaviour of the first two modes in the numerical examples.

The main results of the study can be summarized as follows: (i) a given rotating beam may switch between hardening and softening behaviours when its rotation speed changes. The switching conditions may be depicted on a $\alpha-\beta$ parameter plane to obtain a hardening–softening map of the system (see Fig. 10); (ii) if a beam is under softening conditions, modal amplitude combinations may occur at which a natural frequency vanishes, i.e., vibrations about the trivial equilibrium lose their stability; (iii) a beam exposed to a periodic excitation with varying frequency may experience jump phenomena at the main and (3x) super-harmonic resonances. The same phenomena may also occur under fixed frequency excitation as a result of a change in the rotation speed.

Acknowledgements

The authors are indebted to the reviewers for their helpful comments that contributed to the improvement of the paper. The proofs given in Eqs. (B.8)–(B.12) of Appendix B are contributed by one of the anonymous reviewers.

The first author wishes to express his thanks to the students of his graduate course Nonlinear Oscillations, who have worked out some of the problems in Section 3 as homeworks. The neat work of Mrs. Özge Özdemir Özgümüş, MSc, is especially acknowledged.

Appendix A

The nonlinear equation of motion of the moderately large amplitude transverse vibrations of a stationary, inextensible Euler–Bernouilli beam of flexural rigidity EI, cross-sectional area A, mass density ρ and length ℓ, acted upon by a distributed force with components $f_x(s,t)$ and $f_y(s,t)$ (inertia forces included), and a tip force with components $F_x(t)$ and $F_y(t)$ (Fig. A1) will be derived. To this end, recall first that the bending moment at a station s of a beam at a time t of its motion can be written

$$M(s,t) = \kappa(s,t)EI, \tag{A.1}$$

where the curvature $\kappa(s,t)$ is given by $\kappa(s,t) = \sqrt{(\partial^2 x/\partial s^2)^2 + (\partial^2 y/\partial s^2)^2}$. Noting from the related detail given in Fig. A1 that for an inextensible beam $(\partial x/\partial s)^2 + (\partial y/\partial s)^2 = 1$, one has

$$\frac{\partial x}{\partial s} = \sqrt{1 - \left(\frac{\partial y}{\partial s}\right)^2} \cong 1 - \frac{1}{2}\left(\frac{\partial y}{\partial s}\right)^2, \tag{A.2}$$

so that

$$\kappa(s,t) = \frac{\dfrac{\partial^2 y}{\partial s^2}}{\sqrt{1 - \left(\dfrac{\partial y}{\partial s}\right)^2}} \cong \frac{\partial^2 y}{\partial s^2}\left(1 + \frac{1}{2}\left(\frac{\partial y}{\partial s}\right)^2\right), \tag{A.3}$$

where binome series are invoked and terms higher than the third order are neglected.

On the other hand, making use of Eq. (A.2), the position, velocity and acceleration vectors of a point s of the beam can be expressed:

$$\mathbf{r}(s,t) = \int_0^s \frac{x(\sigma,t)}{\partial\sigma}\mathrm{d}\sigma \cdot \mathbf{i} + y(s,t)\cdot\mathbf{j} \cong \int_0^s \left[1 - \frac{1}{2}\left(\frac{\partial y(\sigma,t)}{\partial\sigma}\right)^2\right]\mathrm{d}\sigma\cdot\mathbf{i} + y(s,t)\cdot\mathbf{j}, \tag{A.4}$$

$$\frac{\partial \mathbf{r}(s,t)}{\partial t} \cong -\int_0^s \frac{\partial y(\sigma,t)}{\partial\sigma}\frac{\partial^2 y(\sigma,t)}{\partial\sigma\,\partial t}\mathrm{d}\sigma\cdot\mathbf{i} + \frac{\partial y(s,t)}{\partial t}\cdot\mathbf{j}, \tag{A.5}$$

$$\frac{\partial^2 \mathbf{r}(s,t)}{\partial t^2} \cong -\int_0^s \left[\left(\frac{\partial^2 y(\sigma,t)}{\partial\sigma\,\partial t}\right)^2 + \frac{\partial y(\sigma,t)}{\partial\sigma}\frac{\partial^3 y(\sigma,t)}{\partial\sigma\,\partial t^2}\right]\mathrm{d}\sigma\cdot\mathbf{i} + \frac{\partial^2 y(s,t)}{\partial t^2}\cdot\mathbf{j}, \tag{A.6}$$

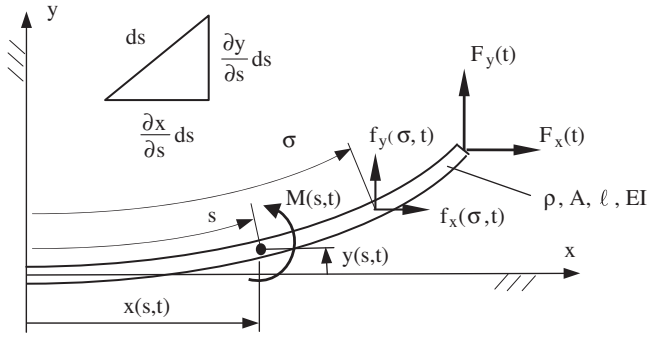

Fig. A1. Stationary, inextensible Euler–Bernouilli beam.

where σ is a dummy variable standing for s. Using Eq. (A.6), the inertial force components can be put apart in the distributed force expressions,

$$f_x(s,t)=\overline{f}_x(s,t)+\rho A\int_0^s\left(\left(\frac{\partial^2 y(\sigma,t)}{\partial\sigma\,\partial t}\right)^2+\frac{\partial y(\sigma,t)}{\partial\sigma}\frac{\partial^3 y(\sigma,t)}{\partial\sigma\,\partial t^2}\right)\mathrm{d}\sigma,$$

$$f_y(s,t)=\overline{f}_y(s,t)-\rho A\frac{\partial^2 y(s,t)}{\partial t^2}, \tag{A.7}$$

where now $\overline{f}_x(s,t)$ and $\overline{f}_y(s,t)$ are either given forces or further inertia forces resulting from a possible overall motion of the beam. The bending moment $M(s,t)$ acting at a point s of the beam can be expressed, in view of Fig. A1, as

$$\begin{aligned}M(s,t)=&-F_x(t)\left[\int_s^\ell\frac{\partial y}{\partial\eta}\mathrm{d}\eta\right]-\int_s^\ell\left\{\left[\bar{f}_x(\sigma,t)+\rho A\int_0^\sigma\left(\left(\frac{\partial^2 y}{\partial\xi\partial t}\right)^2+\frac{\partial y}{\partial\xi}\frac{\partial^3 y}{\partial\xi\partial t^2}\right)\mathrm{d}\xi\right]\left[\int_s^\sigma\frac{\partial y}{\partial\eta}\,\mathrm{d}\eta\right]\right\}\mathrm{d}\sigma\\&+F_y(t)\left[\int_s^\ell\left(1-\frac{1}{2}\left(\frac{\partial y}{\partial\eta}\right)^2\right)\mathrm{d}\eta\right]+\int_s^\ell\left\{\left[\bar{f}_y(\sigma,t)-\rho A\frac{\partial^2 y}{\partial t^2}\right]\left[\int_s^\sigma\left(1-\frac{1}{2}\left(\frac{\partial y}{\partial\eta}\right)^2\right)\mathrm{d}\eta\right]\right\}\mathrm{d}\sigma,\end{aligned} \tag{A.8}$$

where Eqs. (A.7) are used for the distributed forces, ξ, η and σ are dummy variables standing for s, and the integrals with respect to η represent the moment arms of the related forces, calculated by using Eq. (A.2). Now, insert Eqs. (A.3) and (A.8) into Eq. (A.1), take the second partial derivative with respect to s by using the Leibniz rule and obtain

$$\begin{aligned}&\rho A\left\{\left[1-\frac{1}{2}\left(\frac{\partial y}{\partial s}\right)^2\right]\frac{\partial^2 y}{\partial t^2}+\frac{\partial y}{\partial s}\frac{\partial^2 y}{\partial s^2}\int_s^\ell\frac{\partial^2 y}{\partial t^2}\mathrm{d}\sigma+\frac{\partial y}{\partial s}\int_0^s\left[\left(\frac{\partial^2 y}{\partial\sigma\,\partial t}\right)^2+\frac{\partial y}{\partial\sigma}\frac{\partial^3 y}{\partial\sigma\,\partial t^2}\right]\mathrm{d}\sigma\right.\\&\left.-\frac{\partial^2 y}{\partial s^2}\int_s^\ell\int_0^\sigma\left[\left(\frac{\partial^2 y}{\partial\eta\,\partial t}\right)^2+\frac{\partial y}{\partial\eta}\frac{\partial^3 y}{\partial\eta\,\partial t^2}\right]\mathrm{d}\eta\,\mathrm{d}\sigma\right\}+EI\left[\left[1+\frac{1}{2}\left(\frac{\partial y}{\partial s}\right)^2\right]\frac{\partial^4 y}{\partial s^4}+3\frac{\partial y}{\partial s}\frac{\partial^2 y}{\partial s^2}\frac{\partial^3 y}{\partial s^3}+\left(\frac{\partial^2 y}{\partial s^2}\right)^3\right]\\&-\frac{\partial^2 y}{\partial s^2}\left(F_x+\int_s^\ell\overline{f}_x(\sigma,t)\,\mathrm{d}\sigma\right)-\frac{\partial y}{\partial s}\frac{\partial^2 y}{\partial s^2}\left(F_y+\int_s^\ell\overline{f}_y(\sigma,t)\,\mathrm{d}\sigma\right)+\overline{f}_x(s,t)\frac{\partial y}{\partial s}-\overline{f}_y(s,t)\left[1-\frac{1}{2}\left(\frac{\partial y}{\partial s}\right)^2\right]=0\end{aligned} \tag{A.9}$$

as the nonlinear integro-partial differential equation of the transverse vibrations of a stationary, inextensible Euler–Bernouilli beam subjected to a distributed force and a tip force. (The y component of the tip force, if any, need also be considered in the boundary conditions.) Let one note that the involved inextensibility assumption (neither longitudinal vibrations nor elongations due to acting forces are allowed) restricts the use of Eq. (A.9) to beams whose extensional rigidity is considerably higher than its flexural one.

Setting the tip force components to zero in Eq. (A.9) one obtains Eq. (1) above.

Appendix B

The definitions of the coefficients used in Eq. (8) are given below.

$$A_{ij}=\int_0^1[(1-u)\varphi_j''-\varphi_j']\varphi_i\,\mathrm{d}u, \tag{B.1}$$

$$B_{ij}=\int_0^1\left[\frac{1}{2}(1-u^2)\varphi_j''-u\varphi_j'\right]\varphi_i\,\mathrm{d}u, \tag{B.2}$$

$$G_{ijk}=\int_0^1\left(\varphi_j'\varphi_k-\int_0^u\varphi_j'\varphi_k'\,\mathrm{d}\sigma-\varphi_j''\int_u^1\varphi_k\,\mathrm{d}\sigma\right)\varphi_i\,\mathrm{d}u, \tag{B.3}$$

$$C_{ijk\ell} = \int_0^1 \left(\varphi_j' \int_0^u \varphi_k' \varphi_\ell' \, d\sigma + \varphi_j' \varphi_k'' \int_u^1 \varphi_\ell \, d\sigma - \varphi_j'' \int_u^1 \int_0^\sigma \varphi_k' \varphi_\ell' \, d\eta \, d\sigma - \frac{1}{2} \varphi_j' \varphi_k' \varphi_\ell \right) \varphi_i \, du, \tag{B.4}$$

$$D_{ijk\ell} = \int_0^1 \left(\varphi_j' \int_0^u \varphi_k' \varphi_\ell' \, d\sigma - \varphi_j'' \int_u^1 \int_0^\sigma \varphi_k' \varphi_\ell' \, d\eta \, d\sigma \right) \cdot \varphi_i \, du, \tag{B.5}$$

$$E_{ijk\ell} = \int_0^1 \left(\frac{1}{2} \varphi_j^{iv} \varphi_k' \varphi_\ell' + 3 \varphi_j' \varphi_k'' \varphi_\ell''' + \varphi_j'' \varphi_k'' \varphi_\ell'' \right) \varphi_i \, du, \tag{B.6}$$

$$F_{ijk\ell} = \int_0^1 \left(\frac{1}{2} \varphi_j' \int_0^u \varphi_k' \varphi_\ell' \, d\sigma + \varphi_j' \varphi_k'' \int_u^1 \varphi_\ell \, d\sigma - \frac{1}{2} \varphi_j'' \int_u^1 \int_0^\sigma \varphi_k' \varphi_\ell' \, d\eta \, d\sigma - \frac{1}{2} \varphi_j \varphi_k' \varphi_\ell' \right) \varphi_i \, du, \tag{B.7}$$

where φ_i's must be substituted from Eq. (7). Certain properties of these coefficients can be deduced from their definitions above by using the relation

$$\varphi_i^{iv} = \lambda_i^4 \varphi_i \tag{B.8}$$

and the boundary conditions

$$\varphi_i(0) = \varphi_i'(0) = \varphi_i''(1) = \varphi_i'''(1) = 0. \tag{B.9}$$

$A_{ij} = A_{ji}$, $B_{ij} = B_{ji}$and $A_{ii} < 0$, $B_{ii} < 0$. Consider Eqs. (B.1) and (B.2), integrate by parts and use Eq. (B.9) to obtain

$$A_{ij} = \int_0^1 [(1-u)\varphi_j'' - \varphi_j'] \varphi_i \, du = -\int_0^1 (1-u) \varphi_i' \varphi_j' \, du, \tag{B.10}$$

$$B_{ij} = \int_0^1 \left[\frac{1}{2}(1-u^2)\varphi_j'' - u\varphi_j' \right] \varphi_i \, du = -\int_0^1 \frac{1}{2}(1-u^2) \varphi_i' \varphi_j' \, du, \tag{B.11}$$

from which the symmetry property of A_{ij} and B_{ij} immediately follow. Furthermore, the negativity of A_{ii} and B_{ii} follows from the non-negativity of the integrand throughout the integration domain in these equations with $j = i$.

$G_{iji} = 0$. Considering Eq. (B.3) with $k = i$, making use of Eq. (B.8) and applying integration by parts with Eq. (B.9) in mind one has,

$$\begin{aligned} G_{iji} &= \int_0^1 \left(\varphi_i \varphi_j' - \int_0^u \varphi_i' \varphi_j' \, d\sigma \right) \frac{\varphi_i^{iv}}{\lambda_i^4} du - \int_0^1 \left(\varphi_j'' \int_u^1 \frac{\varphi_i^{iv}}{\lambda_i^4} d\sigma \right) \varphi_i \, du \\ &= \frac{1}{\lambda_i^4} \left\{ \int_0^1 \left(\int_0^u \varphi_i \varphi_j'' \, d\sigma \right) \varphi_i^{iv} \, du + \int_0^1 \varphi_i \varphi_j'' \varphi_i''' \, du \right\} \\ &= \frac{1}{\lambda_i^4} \int_0^1 (-\varphi_i \varphi_j'' \varphi_i''' + \varphi_i \varphi_j'' \varphi_i''') \, du = 0. \end{aligned} \tag{B.12}$$

To give an impression on some properties of certain other coefficients referred to in the text, namely; $C_{iiii} > 0$, $E_{iiii} > 0$, $F_{1111} < 0$, $F_{jjjj} > 0$, $j = 2,3,\ldots$, calculated values of a few of these coefficients are given in Table B1.

Table B1
Some calculated coefficients.

i	C_{iiii}	E_{iiii}	F_{iiii}
1	2.143318	10.110166	−0.155068
2	123.998100	3354.524848	51.635317
3	947.739848	66091.373436	447.826090
4	3876.059607	482026.290832	1888.565076
5	11044.253736	2136956.039573	5441.878331

Appendix C

Applying the projection described in Eq. (48) one can calculate the coefficients of Eq. (49). The definitions of those needed in Eq. (50) are given below:

$$c_{iiii} = C_{iiii}u_i^{(i)^4} + (C_{jiiii} + C_{ijii} + C_{iiji} + C_{iiij})u_i^{(i)^3}u_j^{(i)} + (C_{iijj} + C_{jjii} + C_{ijji} + C_{jiij} + C_{ijij} + C_{jiji})u_i^{(i)^2}u_j^{(i)^2} + (C_{ijjj} + C_{jijj} + C_{jjij} + C_{jjji})u_i^{(i)}u_j^{(i)^3} + C_{jjjj}u_j^{(i)^4}, \tag{C.1}$$

$$c_{ijji} = u_i^{(i)^2}[C_{iiii}u_i^{(j)^2} + (C_{ijii} + C_{iiji})u_i^{(j)}u_j^{(j)} + C_{ijji}u_j^{(j)^2}] + u_j^{(i)^2}[C_{jiij}u_i^{(j)^2} + (C_{jjij} + C_{jiij})u_i^{(j)}u_j^{(j)} + C_{jjjj}u_j^{(j)^2}] + u_i^{(i)}u_j^{(i)}[(C_{iiij} + C_{jiii})u_i^{(j)^2} + (C_{iijj} + C_{ijij} + C_{jjii} + C_{jiji})u_i^{(j)}u_j^{(j)} + (C_{ijjj} + C_{jjji})u_j^{(j)^2}], \tag{C.2}$$

$$c_{iijj} = (2C_{ijji} + 2C_{jiij} + C_{iijj} + C_{ijij} + C_{jjii} + C_{jiji})u_i^{(i)}u_j^{(i)}u_i^{(j)}u_j^{(j)} + (2C_{jiiii} + C_{iiji} + C_{ijii})u_i^{(i)}u_j^{(i)}u_i^{(j)^2} + (2C_{ijjj} + C_{jjij} + C_{jiij})u_i^{(i)}u_j^{(i)}u_j^{(j)^2} + (2C_{iiij} + C_{iiji} + C_{ijii})u_i^{(i)^2}u_j^{(j)}u_j^{(j)} + (2C_{jjji} + C_{jjij} + C_{jiij})u_j^{(i)^2}u_i^{(j)}u_j^{(j)} + (C_{iijj} + C_{ijij})u_i^{(i)^2}u_j^{(j)^2} + (C_{jjii} + C_{jiji})u_j^{(i)^2}u_i^{(j)^2} + 2C_{jjjj}u_j^{(i)^2}u_j^{(j)^2} + 2C_{iiii}u_i^{(i)^2}u_i^{(j)^2}, \tag{C.3}$$

$$d_{iiii} = D_{iiii}u_i^{(i)^4} + 4D_{iiij}u_i^{(i)^3}u_j^{(i)} + (2D_{iijj} + 4D_{ijij})u_i^{(i)^2}u_j^{(i)^2} + 4D_{ijjj}u_i^{(i)}u_j^{(i)^3} + D_{jjjj}u_j^{(i)^4}, \tag{C.4}$$

$$d_{iijj} = D_{iiii}u_i^{(i)^2}u_i^{(j)^2} + D_{iijj}(u_i^{(i)^2}u_j^{(j)^2} + u_j^{(i)^2}u_i^{(j)^2}) + D_{jjjj}u_j^{(i)^2}u_j^{(j)^2} + 2(u_j^{(i)}u_i^{(j)} + u_i^{(i)}u_j^{(j)})(D_{iiij}u_i^{(i)}u_i^{(j)} + D_{ijjj}u_j^{(i)}u_j^{(j)}) + 4D_{ijij}(u_i^{(i)}u_j^{(i)}u_i^{(j)}u_j^{(j)}), \tag{C.5}$$

$$e_{iiii} = E_{iiii}u_i^{(i)^4} + (\overline{E}_{iiij} + E_{jiii})u_i^{(i)^3}u_j^{(i)} + (\overline{E}_{iijj} + \overline{E}_{jjii})u_i^{(i)^2}u_j^{(i)^2} + (\overline{E}_{jjji} + E_{ijjj})u_i^{(i)}u_j^{(i)^3} + E_{jjjj}u_j^{(i)^4}, \tag{C.6}$$

$$e_{iijj} = 3[u_i^{(i)}u_i^{(j)^2}(u_i^{(i)}E_{iiii} + u_j^{(i)}E_{jiii}) + u_j^{(i)}u_j^{(j)^2}(u_j^{(i)}E_{jjjj} + u_i^{(i)}E_{ijjj})] + u_i^{(i)}u_j^{(j)}(u_i^{(i)}u_j^{(j)} + 2u_j^{(i)}u_i^{(j)})\overline{E}_{iijj} + u_j^{(i)}u_j^{(j)}(u_i^{(i)}u_j^{(j)} + 2u_j^{(i)}u_i^{(j)})\overline{E}_{jjji} + u_j^{(i)}u_i^{(j)}(u_j^{(i)}u_i^{(j)} + 2u_i^{(i)}u_j^{(j)})\overline{E}_{jjii} + u_i^{(i)}u_i^{(j)}(u_j^{(i)}u_i^{(j)} + 2u_i^{(i)}u_j^{(j)})\overline{E}_{iiij}, \tag{C.7}$$

$$f_{iiii} = F_{iiii}u_i^{(i)^4} + (\overline{F}_{iiij} + F_{jiii})u_i^{(i)^3}u_j^{(i)} + (\overline{F}_{iijj} + \overline{F}_{jjii})u_i^{(i)^2}u_j^{(i)^2} + ([F]_{jjji} + F_{ijjj})u_i^{(i)}u_j^{(i)^3} + F_{jjjj}u_j^{(i)^4}, \tag{C.8}$$

$$f_{iijj} = 3[u_i^{(i)}u_i^{(j)^2}(u_i^{(i)}F_{iiii} + u_j^{(i)}F_{jiii}) + u_j^{(i)}u_j^{(j)^2}(u_j^{(i)}F_{jjjj} + u_i^{(i)}F_{ijjj})] + u_i^{(i)}u_j^{(j)}(u_i^{(i)}u_j^{(j)} + 2u_j^{(i)}u_i^{(j)})\overline{F}_{iijj} + u_j^{(i)}u_j^{(j)}(u_i^{(i)}u_j^{(j)} + 2u_j^{(i)}u_i^{(j)})\overline{F}_{jjji} + u_j^{(i)}u_i^{(j)}(u_j^{(i)}u_i^{(j)} + 2u_i^{(i)}u_j^{(j)})\overline{F}_{jjii} + u_i^{(i)}u_i^{(j)}(u_j^{(i)}u_i^{(j)} + 2u_i^{(i)}u_j^{(j)})\overline{F}_{iiij}, \tag{C.9}$$

where the definitions of Eqs. (41), (42), (44)–(46), and (B.4)–(B.7) must be substituted.

References

[1] R.V. Southwell, F. Gaugh, The free transverse vibration of airscrew blades, British A.R.C. Report and Memoranda No. 766, 1921.
[2] D.A. Peters, An approximate solution for the free vibrations of rotating uniform cantilever beams, NASA TMX-62, 299, 1973.
[3] C.H.J. Fox, J.S. Burdess, The natural frequencies of a thin rotating cantilever with offset root, *Journal of Sound and Vibration* 65 (2) (1979) 151–158.
[4] A.D. Wright, C.E. Smith, R.W. Tresher, J.L.C. Wang, Vibration modes of centrifugally stiffened beams, *Journal of Applied Mechanics* 49 (1982) 197–202.
[5] S. Naguleswaran, Lateral vibration of a centrifugally tensioned uniform Euler–Bernouilli beam, *Journal of Sound and Vibration* 176 (5) (1994) 613–624.
[6] S. Naguleswaran, Out-of-plane vibration of a uniform Euler–Bernouilli beam attached to the inside of a rotating rim, *Journal of Sound and Vibration* 200 (1) (1997) 63–81.

[7] J.S. Rao, W. Carnegie, Non-linear vibrations of rotating cantilever beams, *The Aeronautical Journal of the Royal Aeronautical Society* 74 (1970) 161–165.
[8] J.S. Rao, W. Carnegie, Non-linear vibrations of rotating cantilever blades treated by the Ritz averaging process, *Aeronautical Journal* (1972) 566–569.
[9] K.A. Ansari, Nonlinear flexural vibrations of a rotating Myklestad beam, *AIAA Journal* 12 (1) (1974) 98–99.
[10] K.A. Ansari, Nonlinear flexural vibrations of a rotating pretwisted beam, *Computers & Structures* 5 (1975) 101–118.
[11] P. Gross, M. Gürgöze, W. Kliem, Bifurcation and stability analysis of a rotating beam, *Quarterly of Applied Mathematics* 51 (4) (1993) 701–711.
[12] M. Brons, W. Kliem, Nonlinear analysis of the buckling and vibration of a rotating elasticum, *International Journal of Mechanical Sciences* 36 (7) (1994) 673–681.
[13] E. Peshek, C. Pierre, S.W. Shaw, Modal reduction of a nonlinear rotating beam through nonlinear normal modes, *Journal of Vibration and Acoustics* 124 (2002) 229–236.
[14] M. Abolghasemi, M.A. Jalali, Attractors of a rotating viscoelastic beam, *International Journal of Nonlinear Mechanics* 38 (2003) 739–751.
[15] M.N. Hamdan, B.O. Al-Bedoor, Non-linear free vibrations of a rotating flexible arm, *Journal of Sound and Vibration* 242 (5) (2001) 839–853.
[16] J.W. Larsen, S.R.K. Nielsen, Non-linear dynamics of wind turbine wings, *International Journal of Nonlinear Mechanics* 41 (2006) 629–643.
[17] J.W. Larsen, S.R.K. Nielsen, Non-linear parametric instability of wind turbine wings, *Journal of Sound and Vibration* 299 (2007) 64–82.
[18] G. Bulut, Ö. Turhan, Nonlinear vibrations of rotor-blade systems: modelling, frequency analysis and chaos, *Proceedings of the 15th National Congress on Mechanics*, 2007, pp. 235–244 (in Turkish).
[19] N. Mostaghel, I. Tadjbakhsh, Buckling of rotating rods and plates, *International Journal of Mechanical Sciences* 15 (1973) 429–434.
[20] A. Peters, D.H. Hodges, In-plane vibration and buckling of a rotating beam clamped off the axis of rotation, *Journal of Applied Mechanics* 47 (1980) 398–402.
[21] Ö. Turhan, G. Bulut, Dynamic stability of rotating blades (beams) eccentrically clamped to a shaft with fluctuating speed, *Journal of Sound and Vibration* 280 (2005) 945–964.
[22] J.D. Cole, J. Kevorkian, Uniformly valid asymptotic approximations for certain non-linear differential equations, in: S. Lefschetz (Ed.), *Nonlinear Differential Equations*, Academic Press, New York, 1963, pp. 113–120.
[23] A.H. Nayfeh, D.T. Mook, *Nonlinear Oscillations*, Wiley, New York, 1979.
[24] L. Meirovitch, *Elements of Vibration Analysis*, second ed., McGraw-Hill, New York, 1986.
[25] J. Awrejcewicz, V.A. Krysko, *Introduction to Asymptotic Methods*, Chapman & Hall/CRC, London, 2006.